PUBLICATIONS OF THE ASTRONOMICAL SOCIETY OF THE PACIFIC, **111**:1–30, 1999 January

Invited Review

The Ultraviolet and Optical Continuum Emission in Active Galactic Nuclei: The Status of Accretion Disks

ANURADHA KORATKAR

Space Telescope Science Institute, Baltimore, MD 21218; koratkar@stsci.edu

AND

OMER BLAES

Physics Department, University of California, Santa Barbara, CA 93106; blaes@vela.physics.ucsb.edu

Received 1998 September 29; accepted 1998 October 2

ABSTRACT. A fundamental component of models of active galactic nuclei (AGNs) is an accretion disk around a supermassive black hole. However, the nature of this accretion disk is not well understood, and current models do not provide a satisfactory explanation of the optical/UV continuum observed in AGNs. In this paper we review the substantial theoretical and observational progress made in the field. We also try to point out future research directions that would be fruitful in trying to obtain a complete, self-consistent model of the continuum-emitting regions.

1. INTRODUCTION

Active galactic nuclei (AGNs) are galaxies whose nuclei are highly luminous, with spectra showing broad emission lines covering a wide range of ionization. AGN activity spans a broad range of luminosity, from the brightest quasi-stellar objects (QSOs) to the more common but less luminous Seyfert galaxies. Two significant facts about AGNs make them very interesting to study. The first is their ability to generate extraordinary luminosities (up to 10^{47} ergs s^{-1}) in tiny volumes ($\lesssim 2 \times 10^{14}$ cm; see, e.g., Edelson et al. 1996). The second is the similarity in their spectral features over 7 orders of magnitude in luminosity, across most of the electromagnetic spectrum. No other phenomena have these unusual properties. The similarity in spectral properties over many orders of luminosity indicates that the central engine in AGNs must have the ability to scale with luminosity. It is widely believed that accretion of gas into a central supermassive black hole lies at the heart of the phenomenon (see, e.g., Rees 1984). The accretion flow is thought to be the source of the X-ray, ultraviolet (UV), and optical continuum emission, which ionizes circumnuclear gas in both the broad-line region and narrow-line legion, and may also be the launch site for winds and jets. Well outside the broad-line region (BLR) lies a dusty torus (or perhaps a warped disk) that obscures some lines of sight to the nucleus and accounts for some of the observed diversity in the AGN phenomenon (Antonucci 1993). Readers interested in a broad overview and introduction to the field of AGNs can find several good textbooks, including Peterson (1997) and Krolik (1999).

The standard picture of the central engine of AGNs now has limited observational support. On the smallest scales from *Hubble Space Telescope* (*HST*) imaging and spectroscopic observations, there is evidence for the existence of massive compact objects at the centers of galaxies (Kormendy et al. 1996a, 1996b, and 1997; van der Marel et al. 1997; Ford et al. 1994; Harms et al. 1994; Macchetto et al. 1997; Bower et al. 1997; van der Marel & van den Bosch 1998; Richstone 1998; Magorrian et al. 1998). Very broad Fe Kα lines observed by the *Advanced Satellite for Cosmology and Astrophysics* (*ASCA*) indicate the presence of gas moving in a relativistic potential well (Tanaka et al. 1995; Mushotzky et al. 1995; Nandra et al. 1997b). On parsec scales, *HST* imaging observations (Walter et al. 1996; Ford et al. 1998) and water megamaser observations of a handful of nearby AGNs show a disk structure, possibly the thick molecular torus (Nakai, Inoue, & Miyoshi 1993; Greenhill et al. 1995; Braatz, Wilson, & Henkel 1997).

Despite the fact that much of the large-scale structure has now been observationally verified, we still do not understand the central engine itself. The main difficulty in achieving this goal is that the central accretion flow, which is responsible for the observed optical, UV, and X-ray spectrum, is too small ($\sim 10 R_G = 5 \times 10^{-5}$ pc for a 10^8 solar mass black hole, where $R_G = GM/c^2$ is the gravitational radius of the black hole) to resolve at the distances of even the nearest AGN. (There is one interesting exception: the Einstein Cross, which we discuss in § 3.6 below.) Therefore, we are forced to rely on theoretical models, their predictions, and comparison with observations in order to make progress.

The theoretical accretion models are distinguished by the assumed flow geometry, the state of the plasma within the flow, and the mechanism whereby gravitational energy is converted into observed radiative and kinetic power. The simplest flow

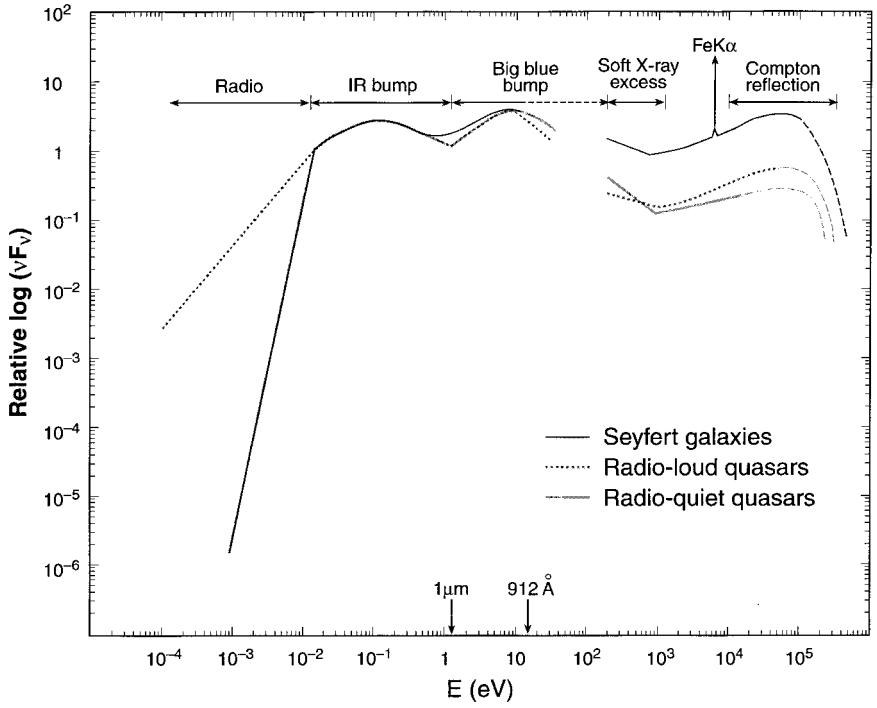

FIG. 1.—Schematic representation of the broadband continuum spectral energy distribution seen in the different types of AGNs. The radio-quiet spectrum can be divided into three major components: the infrared bump, which is thought to arise from reprocessing of the UV emission by dust in a range of temperatures and at a range of distances; the Big Blue Bump, which is directly related to the main energy production mechanism and may be due to an accretion disk; and the X-ray region, which can be interpreted as the high-energy continuation of the Big Blue Bump together with a Comptonized power law with fluorescence and reflection from "cold" material.

geometry is spherical, but such flows are generally very inefficient radiators unless there is some internal source of dissipation, e.g., shocks (Mészáros & Ostriker 1983). Observations on larger scales than the central accretion flow suggest that spherical symmetry is probably broken and that a well-defined axis is present in the central engine. These include the evidence for large-scale gaseous disks as discussed above, as well the presence of jets in both radio-loud and radio-quiet AGNs (Livio 1997; Blundell & Beasley 1998). The axis is generally believed to be associated with the angular momentum of the accretion flow and the hole itself. The specific angular momentum of gas in the central regions of galaxies generally greatly exceeds that of a particle in a circular orbit near the black hole ($\sim R_G c$). To have less than this critical value of angular momentum, material 1 pc away from a $10^8\ M_\odot$ black hole would require nonradial velocity components less than $\simeq 1$ km s^{-1}. Centrifugal forces on material of fixed specific angular momentum vary with radius r as r^{-3}, while gravity varies as r^{-2}. Therefore, unless angular momentum is transported outward on a dynamical timescale as material flows inward from large scales down to the black hole, the flow must become rotationally supported and form an *accretion disk*. As first pointed out by Salpeter (1964) and Zeldovich & Novikov (1964), accretion disks can provide a high efficiency of matter-to-energy conversion in a very small volume. The outward transport of angular momentum occurs slowly through poorly understood dissipative processes ("viscosity"), thereby converting a significant fraction of gravitational energy into heat, magnetic fields, and/or outflowing kinetic energy. It is this largely *theoretical* reasoning that has made disks so ubiquitous as models of the central parts of the accretion flow in AGNs.

The most common assumption about the state of the plasma within the disk is that it is optically thick and thermal. This immediately implies that a substantial fraction of the bolometric power should be in the form of UV photons: a blackbody emitting at a significant fraction of the Eddington luminosity on size scales associated with supermassive black holes has a temperature in the UV range. In fact, a lot of power in AGNs is emitted in the optical/UV region of the spectrum (the Big Blue Bump), but the full spectral energy distribution (SED) is rather more complicated than that. As shown in Figure 1, the overall broadband AGN continuum is relatively flat in νF_ν and extends over nearly 7 orders of magnitude in frequency, which implies that approximately the same amount of energy is emitted per decade of frequency. For radio-quiet AGNs, this broadband spectrum can be divided into three major components: the infrared bump, the Big Blue Bump, and the X-ray region.

The Big Blue Bump (BBB) continuum component in AGNs

extends from the near-infrared at 1 μm to past 1000 Å in the UV and in some cases apparently all the way to the soft X-ray region of the spectrum. More than half the bolometric luminosity of an unobscured AGN is typically emitted within this spectral range, and thus its origin is directly related to the main energy production mechanism. The BBB is thought to arise from an accretion disk and is the spectral region that we will mostly be discussing in this paper. We discuss the observed properties of the BBB extensively in § 3.

The broad infrared bump extends from ~100 to ~1 μm. Quasars show a deep minimum at 1 μm and have a sharp cutoff in the submillimeter. In Seyfert galaxies, the 1 μm minimum is rarely detected because of galaxy starlight contamination (Neugebauer et al. 1987; Sanders et al. 1989). Prior to longer wavelength observations, it was thought that the near-infrared emission in radio-quiet AGNs could be due to synchrotron emission, which could extend as a power law to higher photon energies underneath the BBB. Today, however, the infrared bump is generally thought to arise from reprocessing of the BBB emission by dust with temperature in the range of 10–1800 K and at a range of distances from the central UV source (Barvainis 1987, 1990; Sanders, Scoville, & Soifer 1988; Phinney 1989). The spectral trough at 1 μm is then naturally interpreted as being due to the finite sublimation temperature (~1800 K) of dust. Additional evidence for the dust interpretation is the fact that the infrared hump shows no rapid variability (see, e.g., Hunt et al. 1994) and that the long-wavelength turnover in the submillimeter is very steep (see, e.g., Hughes et al. 1993). Observations of a handful of radio-quiet AGNs in the far-infrared using the *Infrared Space Observatory* show strong evidence for thermal emission (Haas et al. 1998). In the radio-loud AGNs, the infrared emission is a mixture of thermal and nonthermal radiation, but in most cases one of the two components is dominant (Haas et al. 1998).

In the soft X-ray region, many objects show a "soft X-ray excess," which is emission that exceeds the extrapolation from the observed hard X-ray power-law continuum (Turner & Pounds 1989; Masnou et al. 1992). This excess is subject to a number of observational difficulties and is probably the least well understood component of the AGN's spectral energy distribution (SED). It may be that it is the high-energy continuation of the BBB, but this interpretation is not straightforward. We discuss the details in § 3.1 below. The characteristics of the soft X-ray excess in both Seyfert galaxies and quasars are not well quantified. Radio-quiet QSOs have a mean energy spectral index ($F_\nu \propto \nu^{\alpha_X}$) of $\alpha_X = -1.72 \pm 0.09$ in the soft X-ray band (Laor et al. 1997), while Seyfert 1 galaxies have $\alpha_X \sim -1.37$ (Turner, George, & Mushotzky 1993; Walter & Fink 1993).

In the hard X-ray band, the AGN spectrum consists of a power law with energy spectral index ~ -0.9. This power law is almost universally believed to be due to Compton upscattering of optical/UV photons by hot or nonthermal electrons somewhere in the central engine, possibly a hot, magnetized corona above the disk. Superposed on this power law are an Fe Kα emission line at 6.4 keV and a Compton reflection hump above 10 keV, at least in the case of some Seyfert galaxies (Pounds et al. 1989; Nandra & Pounds 1994). These two features are thought to be due to fluorescence and reflection from "cold" material, possibly the accretion disk itself in the case of Seyfert 1 galaxies. This is supported by the fact that the Fe Kα emission line is observed to be very broad (Tanaka et al. 1995). Both the reflection hump and the hard X-ray power law extend up to high energies before cutting off at around several hundred keV (Gondek et al. 1996). The hard X-ray properties of high-luminosity AGNs (QSOs) are not as well understood, partly because they are relatively faint in the hard X-rays given their optical/UV luminosity compared to Seyfert galaxies. The Fe Kα line and reflection hump are relatively weak or nonexistent (Iwasawa & Taniguchi 1993; Nandra et al. 1995; Nandra et al. 1997c).

It is the purpose of this paper to review the current status of the observational and theoretical research effort to understand the central accretion flow and its relation to the BBB. We focus almost exclusively on radio-quiet AGNs, whose emission is dominated by the accretion flow. Radio-loud objects can also have substantial contributions to their observed emission from jets and outflows, and we refer the reader to the excellent review of Urry & Padovani (1995) for a discussion of their properties. While we will mention the important clues being provided by other regions of the electromagnetic spectrum, particularly X-rays, we concentrate here on the optical/UV BBB. We begin § 2 of the paper by discussing the early, simple accretion disk models that were first applied to the AGN problem. These models have proved to be very inadequate, and we discuss the main observational problems in § 3. We then turn to more recent efforts to improve these models and how they fare against the observations in § 4. We discuss alternatives to the standard accretion disk paradigm in § 5. Finally, we summarize our main conclusions in § 6, pointing out the main research directions, both theoretical and observational, which we feel will lead to further progress in our understanding of the primary power source of AGNs.

2. EARLY ACCRETION DISK MODELS

Even if one assumes that angular momentum plays an important role in the dynamics of the central accretion flow, the flow geometry is still very uncertain. The simplest assumption that one can make is that the radial dynamics of the flow is dominated by gravitation and rotation, with radiation pressure, gas pressure, and magnetic forces being negligible by comparison. The plasma in the disk then orbits the black hole on nearly circular test particle ("Keplerian") orbits, and the flow takes the form of a geometrically *thin disk*. The vertical extent of this disk is determined by balancing the small (by assumption!) internal pressure of the disk with the small vertical component of gravity from the central black hole. At large radii, self-gravity can also become important. The thin disk assump-

tion necessarily breaks down at high accretion luminosities approaching the Eddington limit, where radiation pressure becomes important. In addition it may not be a good assumption at very low accretion rates. We will discuss these complications further in § 5 below.

The fundamental uncertainty that plagues all theoretical models of accretion disks is the mechanism of outward angular momentum transfer, which is responsible for the slow inward spiral of material that converts gravitational potential energy into radiation and/or an outflow. There are two particularly promising mechanisms for angular momentum transfer in disks, both of which involve magnetic fields. The first is a magnetohydrodynamic (MHD) outflow, where magnetic fields supply torques to the disk and carry away angular momentum in the outflow (Blandford & Payne 1982). The second is internal MHD turbulence, as seen in simulations of the nonlinear development of the Balbus-Hawley instability (Balbus & Hawley 1991; Stone et al. 1996; Balbus & Hawley 1998). Very few models of the radiation produced in the accretion flow are based on these ideas, however, and generally angular momentum transport is treated through a parameterized viscous stress. The most popular prescription is the α-viscosity of Shakura & Sunyaev (1973), in which the radial/azimuthal component of the viscous stress is taken to be a parameter α times the total (gas plus radiation) pressure. We will have very little to say here about the detailed mechanisms whereby gravitational energy is converted to radiative and kinetic power in AGNs. Nevertheless, until this is understood, models and interpretation of observations will be severely handicapped.

The basic theoretical models of stationary, geometrically thin disks around black holes were developed by Shakura & Sunyaev (1973) and Novikov & Thorne (1973) (see also Page & Thorne 1974; Eardley & Lightman 1975; Riffert & Herold 1995; and Abramowicz, Lanza, & Percival 1997 for important corrections and refinements to these fundamental papers). From the point of view of predicting the observed spectrum, such models are the most well constrained of all the possible accretion flows considered to date. They make several key assumptions about the flow. In particular, the disk is stationary and axisymmetric and extends down to the innermost stable circular orbit, where zero stress is assumed to be exerted on the disk. Inside this point material falls quickly into the hole and emits very little radiation. Angular momentum transport within the disk occurs by local "viscous" stresses that convert gravitational energy entirely into heat. Because the disk is thin, this heat is assumed to flow vertically out of the disk, thereby being emitted at the same radius as it was generated. Under these assumptions, the radiative flux emerging from each face of the disk at radius r is given by

$$F(r) = \frac{3GM\dot{M}}{8\pi r^3}\mathcal{I}(r), \qquad (1)$$

where M is the mass of the black hole, $\dot{M}$ is the mass accretion rate, and $\mathcal{I}(r)$ is a correction factor that depends on the mass and angular momentum of the hole and approaches unity at large radii. The local disk flux therefore depends only on the properties of the black hole and the accretion rate. At large radii, $F(r) \propto r^{-3}$, which implies that the effective temperature of the disk surface varies as $T_{\rm eff} \propto r^{-3/4}$.

The geometry of the thin disk allows one to calculate the overall emergent spectrum from this *total* flux by dividing the disk into concentric annuli, calculating the spectrum emitted by each annulus and then summing them all together. The very simplest assumption is that each annulus radiates like a blackbody. The $r^{-3/4}$ effective temperature distribution at large radii then gives a long wavelength SED of $F_\nu \propto \nu^{1/3}$. As we discuss in § 3.1 below, this is much bluer than is typically observed in the optical/UV spectra of AGNs.

Blackbody emission is unlikely to be a good approximation to the spectrum at each radius, even if the disk were optically thick, which it may not be! Careful modeling of the vertical structure and radiative transfer through each annulus is necessary to calculate the overall emitted spectrum. In contrast to the radial structure, the vertical structure of the disk is highly dependent on the assumed mechanism of angular momentum transfer, including *its* vertical dependence. Vertical energy transport can proceed by bulk motions of plasma and magnetic fields as well as by radiation through a supposedly stationary medium. Magnetic and turbulent stresses may well contribute to the vertical pressure support. The disk can be effectively optically thin in the vertical direction, particularly in the innermost regions if the viscosity is high. Even in models in which the disk is optically thick and vertical energy transport occurs through radiation, stellar atmosphere modeling is necessary. In addition to atomic opacity sources, including lines broadened by turbulence, electron scattering (both Thomson and Compton) is crucial in determining both the radiative transfer and the vertical disk structure. High temperatures and low densities mean that many atomic level populations are strongly coupled to the radiation field, and non-LTE effects are important. Illumination of the disk photosphere by external sources of X-ray radiation with significant power is also important, particularly in Seyfert galaxies. Relativistic effects must be included. Gravitational light bending will change the flux distribution through absorption and reprocessing (as will flaring or warping of the outer disk). Corrections must be made for the relativistic "transfer function" (Cunningham 1975; Speith, Riffert, & Ruder 1995; Agol 1997); i.e., the spectrum observed at infinity is altered by Doppler shifts, aberration, gravitational redshifts, and light bending. Radiation from disks around rapidly rotating Kerr holes can also be focused back onto the disk, modifying the emerging spectrum (Cunningham 1976). Given the enormous complexities and uncertainties, it is essential that models pay close attention to, and be guided by, observations.

A crude, first-order modification to the blackbody assumption is to take into account the fact that Thomson scattering

opacity may dominate absorption opacity in the innermost regions of the accretion flow. The spectrum at each annulus may then be crudely modeled as a modified blackbody. This flattens the SED and produces more high-energy photons (Shakura & Sunyaev 1973). This is an important effect in accretion disks around stellar mass black holes, but whether or not it occurs in the disks of AGNs depends on the detailed vertical structure of the disk (see § 4).

Shields (1978) proposed that the optical continuum in AGNs could be due to thermal emission from an accretion disk. He fitted the SED of 3C 273 by a nonthermal power law that extended from the infrared to the X-rays with an additional thermal component in the optical/UV. Thus, the BBB was for the first time associated with thermal accretion disk radiation. The nonthermal continuum prescription continued to be used in later models (Malkan 1983; Sun & Malkan 1989; Laor & Netzer 1989; Laor 1990) to account for the flat optical continua observed in the spectra of AGNs (see § 3.1).

Multiwavelength observations of other AGNs were first compared to accretion disk models by Malkan (1983). In his comparisons, there were three components: a nonthermal infrared–to–X-ray power-law spectrum, a thermal accretion disk spectrum, and a recombination spectrum. The accretion disk models in this early work were just face-on disks in which the emergent flux was described by blackbodies. The models did account for relativistic effects in the disk structure as well as the effects of the relativistic transfer function. The results of this work showed that accretion was at super-Eddington rates in bright QSOs, where the assumptions of these accretion disk models break down. This work also discussed many observational tests for accretion disks. Sun & Malkan (1989) extended this work to include disk inclination angle effects and fitted many more sources. However, the fits relied crucially on the assumption of an underlying infrared power law, and the emergent flux was still approximated by blackbodies.

The earliest attempt at calculating the detailed overall spectrum of optically thick, geometrically thin accretion disks using stellar atmosphere models appropriate for AGNs was by Kolykhalov & Sunyaev (1984). They used the α-viscosity prescription to calculate the vertical structure of each annulus. They then took existing stellar atmosphere models from the libraries existing at that time (e.g., Kurucz 1979) with appropriate surface gravities and effective temperatures and then summed them together to generate overall spectra. The most interesting result of their calculations was the existence of very large absorption edges at the hydrogen Lyman limit—edges that existed even when the smearing effects of the relativistic transfer function were included. As we discuss in § 3.2 below, such edges are not observed, and they noted this discrepancy at the time. This problem motivated much of the later theoretical and observational work on the Lyman edge region of the spectra of AGNs. But as we discuss in § 4, these early calculations suffered from severe limitations.

Because electron-scattering opacity is important in the disk atmosphere at the expected temperatures and densities, the radiation emerging from the disk can be substantially polarized. Most of the early work assumed that the polarization would be similar to that emerging from an optically thick, pure electron-scattering atmosphere. In this case the polarization is perpendicular to the disk axis and has a strong aspect angle dependence, varying from 0% for a face-on disk (because of symmetry) to 11.7% for an edge-on disk (Chandrasekhar 1960; Rees 1975; Lightman & Shapiro 1975). Pioneering work in the 1980s showed that optical polarization in AGNs is generally much lower ($\lesssim$1%) than predicted by these simple models. Often no polarization is detected, and the polarizations are *parallel* to the nuclear axes, when the latter can be inferred from a radio jet position angle (Stockman, Angel, & Miley 1979; Antonucci 1988).

3. OBSERVATIONS

3.1. The Big Blue Bump

To understand the nature of the BBB we first need to determine its SED and thus determine its strength compared to the AGN's SED. Although this task seems relatively simple, there are a lot of observational problems. One of the most important problems is that a substantial part of the BBB in any particular source is in the unobservable part of the electromagnetic spectrum (13.6 eV–0.1 keV), where it is hidden by Galactic absorption. Therefore, the characteristics of this region need to be inferred from theoretical considerations. In the optical/UV wavelength region, where AGNs can be observed, the spectra have the characteristic strong broad emission lines whose wings make assignment of "line-free continuum" regions very difficult. Further, the Balmer continuum and the many blended Fe II emission lines produce a relatively smooth feature in the AGN spectrum that also has to be accounted for in the continuum fitting process (Wills, Netzer, & Wills 1985). Thus, in this section we discuss the shape of the BBB by considering the optical/UV region and the far-UV/soft X-ray regions separately. We also discuss in detail the observational caveats in each spectral region. We will often discuss composite spectra that have been generated by co-adding several hundred optical/UV spectra in the AGN rest frame. These composites serve as a high signal-to-noise ratio reference to the "observed" AGN shape, because although individual AGN spectra differ in detail, they all have similar characteristic features. It is important to remember, however, that *a composite spectrum really has no physical meaning*, and models must be fitted to spectra of individual sources.

3.1.1. The Optical to UV Region

The median optical to UV continuum slope in radio-quiet QSOs is $\alpha \simeq -0.32$ ($F_\nu \propto \nu^\alpha$; Francis et al. 1991). The slope was determined in the 1300–5500 Å region after the Balmer continuum and the Fe II line emission were accounted for in the continuum fitting process. Using *International Ultraviolet*

Explorer (*IUE*) data, O'Brien, Gondhalekar, & Wilson (1988) found that the rest-frame UV slope (1200–1900 Å) is slightly steeper than the optical and that higher luminosity objects have flatter slopes than lower luminosity objects. The rest-frame UV slope (1050–2200 Å) from *HST* data is -0.99 (Zheng et al. 1997). It must be noted here that there is substantial scatter in the slopes of the individual objects, yet the optical/UV continuum is redder than the long wavelength prediction of stationary accretion disk models.

3.1.2. The Far-UV to Soft X-Ray Region

Historically, because a substantial part of this wavelength region is unobservable, there have been two approaches to inferring the BBB shape. In the first approach, the BBB continuum was associated with thermal emission from an accretion disk (Shields 1978; Malkan 1983; Kolykhalov & Sunyaev 1984). In the second approach, the shape of the BBB was obtained by comparing photoionization model predictions with observed emission-line strengths (Mathews & Ferland 1987). Both these approaches indicated that the BBB is energetically very important, peaking in the extreme UV and usually dominating the quasar luminosity (MacAlpine 1981; Czerny & Elvis 1987; Mathews & Ferland 1987; Sun & Malkan 1989; Shields 1989; Laor 1990; Bechtold et al. 1994; Walter et al. 1994).

The two recent *HST* and *Roentgen Satellite* (*ROSAT*) investigations by Zheng et al. (1997) and Laor et al. (1997), respectively, allow us to investigate observationally the "observed" shape of the BBB in the 13.6 eV–1 keV region of the continuum. The UV composite spectrum of Zheng et al. was compiled using *HST* Faint Object Spectrograph (FOS) observations. This sample contained quasars with mean redshifts $\sim$1, which allowed determination of the UV composite spectrum in the rest wavelength range $\sim$300–3000 Å (see Fig. 2). The individual spectra in the composite have been corrected for Galactic reddening and intergalactic absorption. The UV composite spectrum of AGNs does not appear to rise to shorter wavelengths but seems to roll over shortward of 1000 Å. Laor et al. (1997) produced a composite soft X-ray spectrum of a complete sample of low redshift quasars using *ROSAT* Position Sensitive Proportional Counter (PSPC) observations. The soft X-ray data seem to be just an extension of the UV composite spectrum (see Fig. 3). If taken at face value, the UV and X-ray composite spectra indicate that the BBB may not be as energetically dominant as thought previously. Further, the peak of the "observed" BBB does not seem to be in the extreme-UV (100–800 Å) but rather in the far-UV region (900–1100 Å).

3.1.3. Observational Caveats

There are a number of observational issues that can affect the observed shape of the BBB. These issues should especially be kept in mind when considering the shape of the BBB, as determined by the UV and X-ray composite spectra, because they affect each individual object in a different manner and thus possibly create an unphysical effect in the composite spectrum. Below we discuss the various issues in detail.

Host galaxy contamination.—The optical/UV region of an AGN spectrum is also where stars put out most of their radiation. Thus careful galaxy subtraction is necessary if we are to determine the shape of the BBB accurately. In low-redshift AGNs, such corrections are often made by subtracting with galaxy bulge template spectra. However, this may be inadequate because the correction does not effectively correct for a starburst population. *HST* imaging observations of Seyfert galaxies show that nuclear star formation is often occurring well within 0.″5–1.″0 of the nucleus. Depending on the dominance of these star-forming regions, they can contribute substantially toward the optical/UV light that is seen in most ground-based apertures. A comparison of contemporaneous *HST* and ground-based spectroscopy of NGC 7469 clearly shows this problem (see Figs. 4 and 5). In this particular object, $\sim$70% of the starlight falls within 0.″1 of the nucleus! For ground-based observations, this problem is exacerbated owing to effects of seeing. Although nuclear starbursts are likely to be present in the host galaxies of high-luminosity AGNs (QSOs), more than 80% of the radiation is from the QSO. Therefore for these objects we do not expect substantial contamination in the optical/UV region from the host galaxy.

Intrinsic reddening.—Intrinsic reddening in the AGN plays an important role when determining the optical/UV continuum. It is generally assumed that the intrinsic reddening in AGNs is small [$E(B-V) = 0.05$–0.1 mag], independent of the reddening law. Although this small amount of reddening does not affect the optical fluxes dramatically, it has a dramatic effect at UV wavelengths. This reddening correction becomes extremely crucial for high-z AGNs since the reddening correction is applied to the far-UV rest wavelengths. Thus applying a reddening correction, even a very small one, can effectively change the shape of the observed BBB spectrum.

In most analyses the continuum is corrected for Galactic reddening, and there may sometimes be an attempt to correct for intervening intergalactic absorption. An attempt to correct for intrinsic reddening via line ratios is also often made, but depending on the line ratios, one can get significantly differing amounts for the correction. In addition, the reddening might be different for the line- and continuum-emitting regions. A systematic analysis of the reddening indicators and effects of dust in multiwavelength spectra needs to be undertaken, especially now that we have mounting evidence for dust in the nuclei of AGNs (Malkan, Gorjian, & Tam 1998).

The UV composite spectrum generated by Zheng et al. (1997) has a spectral break at 1000 Å. Could this prominent continuum feature be due to inaccurate corrections for intrinsic reddening in each individual AGN? Laor & Draine (1993) have shown that dust opacity peaks at $\sim$700–800 Å and drops sharply at shorter wavelengths. If the far-UV spectral slope change in

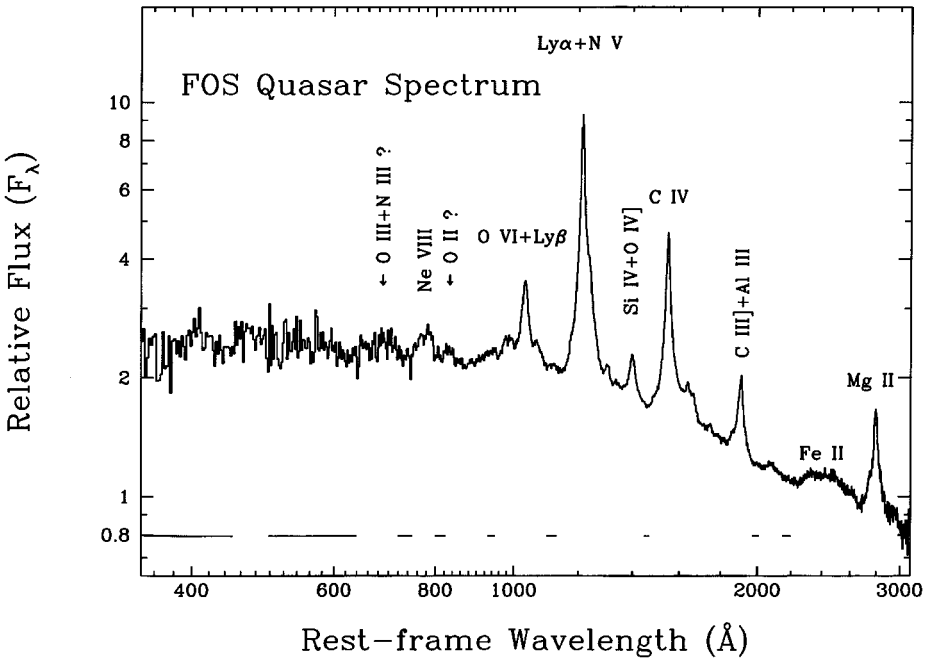

FIG. 2.—UV composite spectrum compiled using *HST*/FOS observations. The individual spectra in the composite have been corrected for Galactic reddening and intergalactic absorption. Note that the composite spectrum does not appear to rise to shorter wavelengths but seems to roll over shortward of 1000 Å. The 1050–2200 Å region can be fitted by a power-law continuum $F_\nu \propto \nu^{-0.99}$. Shortward of 1000 Å, the spectrum in F_ν is close to ν^{-2} and seems to allow a smooth extension into the soft X-rays (courtesy W. Zheng).

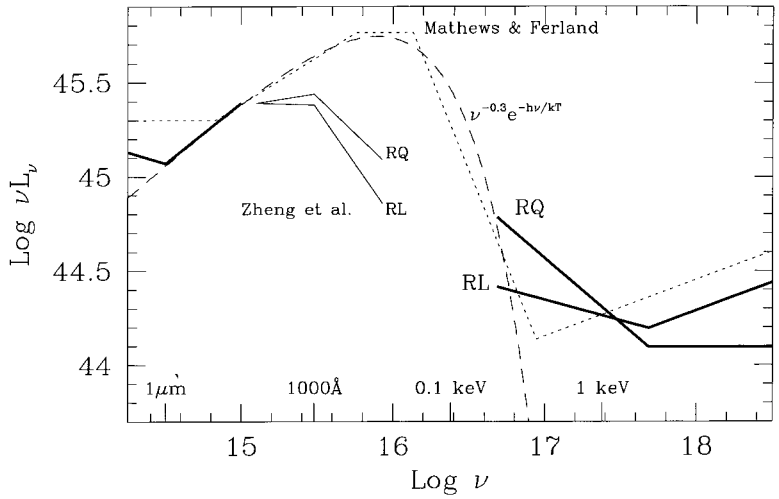

FIG. 3.—Composite "observed" optical–soft X-ray spectrum for AGNs. The composite UV spectra for radio-loud (RL) and radio-quiet (RQ) objects are plotted as a thin solid line. The thick solid lines represent the optical and soft X-ray composite spectra. The dotted line is the spectral shape predicted by Mathews & Ferland (1987), while the dashed line shows a simple power-law model (*not* an accretion disk) with a thermal cutoff corresponding to $T = 5.4 \times 10^5$ K. The data suggest that the far-UV power-law extends into the soft X-ray regime. The 0.2–2.0 keV spectral slope is much flatter than predicted by the simplest thin accretion disk models, which have exponential cutoffs in this wave band (courtesy A. Laor).

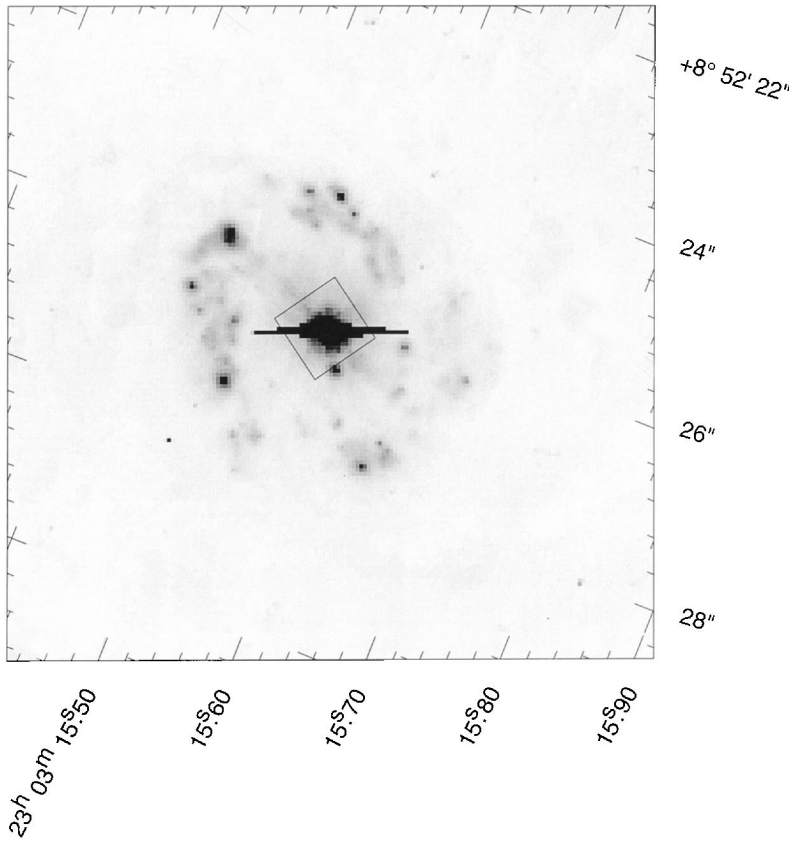

FIG. 4.—The *HST* Wide Field Planetary Camera 2 image of the nuclear region of NGC 7469. The 3″ diameter starburst ring is clearly visible. The nucleus of the galaxy is saturated in this image. Note that in a ground-based slit spectrum, depending on the slit (usually 1″ in width) orientation, the ring contaminates the spectrum. Further, such rings would also have contaminated the UV spectra obtained by *IUE* whose aperture was 10″ × 20″. The square represents the 0.″86 square FOS aperture (courtesy W. Welsh).

the Zheng et al. spectrum was due to dust, then below 700 Å the composite spectrum should have "recovered" by 400 Å. Such a change in continuum slope is not seen, which indicates perhaps that the effects of intrinsic dust reddening are not important. However, it must be noted that the far-UV spectral region of the composite has few objects contributing to the spectrum. These objects are at high redshifts, and their continua have been statistically corrected for intervening intergalactic absorption (for clouds with $N_{\rm H} < 10^{16}$ cm^{-2}), and additional corrections if the objects were known to have intervening absorption systems.

In an individual spectrum, reddening will not cause a spectral break at 1000 Å but will just change the slope of the spectrum dramatically at these short wavelengths. In fact, because of the composite nature of the spectrum, it may be possible that the spectral break is prominent owing to incorrect reddening corrections in each of the individual spectra that extend over limited regions of the entire wavelength range of the composite. Notwithstanding the above observational caveats, the incidence of the spectral break at 1000 Å, so close to the Lyman limit, is tantalizingly suggestive of an intrinsic emission mechanism as the cause.

Extreme-UV energy distribution.—As mentioned earlier, to understand the primary emission mechanism in AGNs, it is crucial to know the shape of the BBB in the extreme-UV (EUV). We have to determine if the UV composite truly represents the EUV SED in AGNs. At wavelengths less than 800 Å, only a few objects are contributing toward the UV composite of Zheng et al. (1997). There are very few observations of AGNs in this region that can be used for a quantitative analysis of the EUV energy distribution. For both Seyfert galaxies and QSOs, there are individual objects in which the BBB SED is not similar to that derived from the UV and X-ray composite spectra (e.g., HS 1700+6416, HS 1103+6416, and HE 2347−4342 from Reimers et al. 1998; PG 1211+14; Zheng et al. 1999). Figure 6 shows the far-UV and EUV SED in luminous AGNs. The variety of the EUV SEDs indicate that describing the BBB with simple models will not be possible and that the task is much more complex, and the SED at these short wavelengths needs to be quantified better.

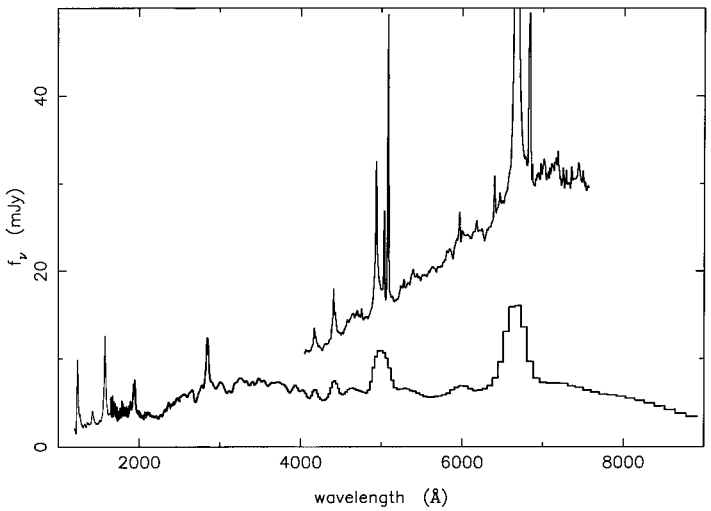

FIG. 5.—Comparison of the contemporaneous *HST*/FOS (*lower curve*) and ground-based spectroscopy of NGC 7469. The *HST*/FOS spectrum is through a 0.″86 square aperture, while the ground-based spectroscopy is mostly through a $10'' \times 16.''8$ slit (similar in size to the *IUE* large-aperture data). The estimated host galaxy contamination is ~18% at 5400 Å, which we see in the figure is highly underestimated. The gross difference between the *HST*/FOS and ground-based fluxes is due to the host galaxy and starburst ring contribution in the ground-based spectrum. This figure highlights the value of high spatial resolution spectroscopy (courtesy W. Welsh).

Soft X-ray issues.—The soft X-ray excess component in AGNs is important for the evaluation of accretion disk models because it is often interpreted as the high-energy tail of the BBB and it helps determine the total energy emitted in the BBB. There are a number of spectral components that contribute to the X-ray excess region (0.1 to ~1 keV), including the underlying X-ray power law and the "warm absorber" (absorption in the 0.5–1.5 keV range dominated by O VII and O VIII K-shell absorption edges in material with $N_{\rm H} \sim 10^{22}$ cm^{-2}). All these spectral components complicate the theoretical interpretation of this region. A detailed analysis of *ASCA* data by George et al. (1998) challenges the presence of the soft X-ray excess in some objects, and recent *BeppoSAX* data fail to show a soft X-ray excess in many sources in which such an excess was claimed to exist before (Matt 1998). The presence of a warm absorber in Seyfert galaxies and the lack of warm absorbers in high-luminosity AGNs has lead to some extent to more observational uncertainty.

To add to the modeling difficulties, simultaneous data obtained with *ASCA* and *ROSAT* showed different slopes in the 0.2–1 keV bands. The soft X-ray slopes observed by Laor et al. (1997) need to be verified because there have been observational issues concerning the accuracy of the *ROSAT* PSPC calibration matrix, especially at low flux levels (which is obviously the case for X-ray observations of AGNs). However, the H I columns determined by Laor et al. agree remarkably well with the accurate 21 cm H I columns, which suggests that the *ROSAT* PSPC calibration matrix may be quiet reliable.

It is difficult to compare the *ROSAT* and *ASCA* observatories. *ASCA* cannot observe the soft X-rays ($\lesssim$0.6 keV) and has a broad wave band (0.4–10 keV) and high energy resolution, while the *ROSAT PSPC* observed soft energies (0.1 keV) but did not have a broad wave band or high energy resolution. The presence of numerous spectral components and their relative contributions at various energy bands further complicates comparisons between the two observatories. Thus, interpretation of the soft X-ray excess depends on our understanding of the broader X-ray wave band.

Sample consistency.—The UV X-ray composite shown in Figure 3 is based on two different samples. The far-UV composite is based mainly on quasars with $z > 1$, while the soft X-ray composite is based exclusively on quasars with $z < 0.4$. Thus, if the quasar SED evolves with z, it may be misleading to combine the SED of high- and low-z samples. One clearly needs to measure the far-UV and soft X-ray continuum for the same population of quasars in order to establish the shape of the BBB.

3.2. Lyman Edges

The accretion disks of AGNs are thought to include thermally radiating regions with temperatures in the range 30,000–300,000 K. A fundamental signature of thermal gas is that the emitted spectrum should show spectral features that are associated with large changes in opacity of the gas. At the expected temperatures and densities of an accretion disk, neutral hydrogen ionizes, and there is a large change in the opacity

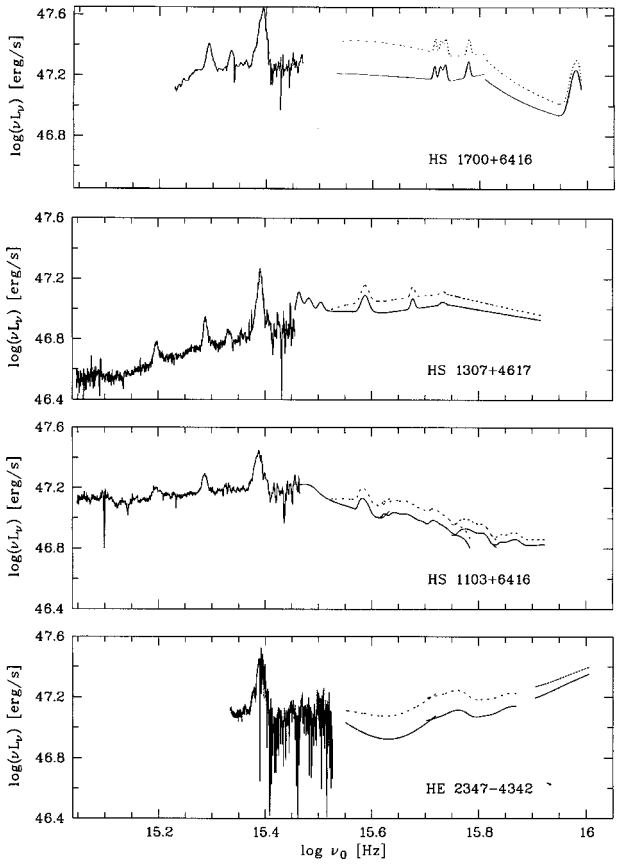

FIG. 6.—Spectral energy distributions for four high-redshift QSOs detected in the Hamburg quasar survey. The spectra are shown in the rest frame of the quasar. The UV continua derived for the dereddened spectra have been corrected for H I continuum absorption of the Lyman limit systems. An additional correction for the cumulative H I continuum absorption of Lyα clouds with $\log N(\mathrm{H\ I}) \leq 16\ \mathrm{cm}^{-2}$ is indicated by the dotted lines. We see that each of these AGNs show dramatically different EUV distributions (courtesy D. Reimers).

of the gas. The ionization of hydrogen should give rise to spectral features at the Lyman limit (912 Å). The SED in the Lyman limit region can therefore be used as an important diagnostic of accretion disk characteristics. The exact nature of the Lyman edge feature, which will be discussed in § 4.2, depends on the viewing angle of the disk, the conditions in the disk atmosphere (e.g., vertical structure of the disk, atomic level populations), the conditions in the accretion system (e.g., the accretion rate, black hole mass), and general relativistic effects.

Since the strength and shape of the Lyman limit feature are diagnostics of the properties of the gas, observational studies have concentrated on quantifying the nature of the spectral feature at the Lyman limit. The Lyman edge region for AGNs has now been investigated at high (Antonucci, Kinney, & Ford 1989), intermediate (Koratkar, Kinney, & Bohlin 1992), and low (Kriss et al. 1996; Kriss et al. 1997; Zheng et al. 1995) redshifts. Figure 7 shows the variety of continuum distributions seen in the Lyman limit region. Of the 73 AGNs investigated in these studies, only eight candidate objects were found that might have an intrinsic Lyman edge that may be associated with an accretion disk. In these candidate "partial" Lyman edge objects, there is *no sharp discontinuity* in the continuum at the Lyman limit but usually just a change in continuum slope on either side of 912 Å (see Fig. 7). In objects in which a sharp Lyman absorption edge is present, nearly 25% of objects investigated, the feature can clearly be associated with intervening absorbing material such as broad emission line clouds in the AGN or gas in the AGN host galaxy. Two (Sun, Malkan, & Chang 1993 and Tytler & Davis 1993) seemingly contradictory results concerning the statistics of Lyman edges in *HST* data have been reported. A uniform detailed analysis needs to be conducted. Analyses so far conclude that intrinsic Lyman edge features that can be associated with accretion disk features are *rare* in AGNs, and more importantly there has been *no* reported case of a Lyman edge feature *in emission*.

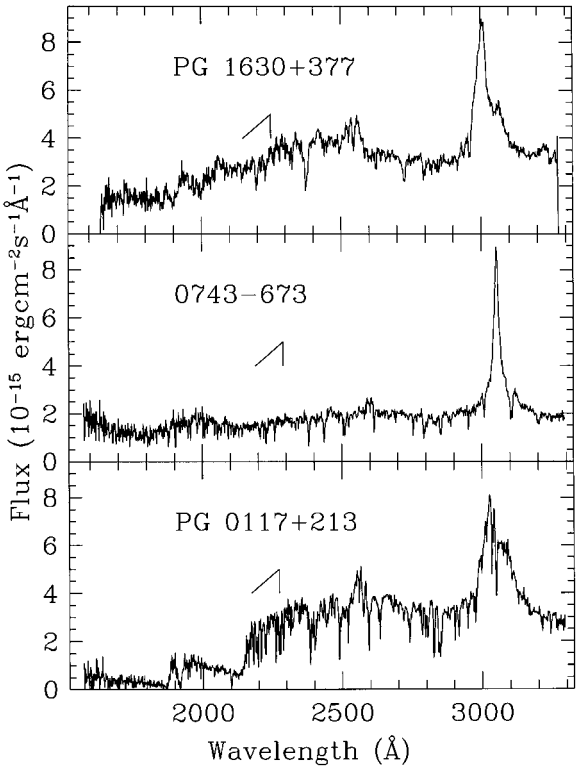

FIG. 7.—Spectral energy distribution in the Lyman limit region. The spectrum of PG 1630+377 (*top panel*) is an example with a possible intrinsic Lyman edge. The Lyman limit in this object shows no sharp discontinuity like that seen in PG 0117+213 (*bottom panel*) but does show a change in slope on either side of the Lyman limit. The spectrum of 0743−673 (*middle panel*) is an example in which we see no Lyman edge. The spectrum of PG 0117+213 (*bottom panel*) shows sharp Lyman edges at ~850 Å and ~750 Å owing to intervening absorbing material. The location of the intrinsic Lyman limit is indicated by the arrows in each panel.

On a statistical basis, one could use the UV composite spectrum (Zheng et al. 1997) to determine the nature of the Lyman edge. In this spectrum the edge is seen only as a 10% effect (see Fig. 8). This may be indicating that many AGNs have a very weak Lyman edge feature. But given the fact that intrinsic Lyman forest lines and reddening can have a dramatic effect on the correction for the SED in this region, the 10% effect cannot be used effectively to quantify the nature of the spectral feature at the Lyman limit.

To investigate the Lyman edge in AGNs, the observational studies have been over a limited wavelength region in both low-redshift and high-redshift objects. Since the accretion disk is in the black hole environment, the Lyman edge is expected to be broadened by disk rotation and by general relativistic effects (owing to the extreme depth of the local potential). Testing the theoretical models would ideally involve high signal-to-noise ratio observations over a wavelength range ~450 to ~1200 Å in the AGN rest frame. This is observationally extremely difficult because complete access to this region at low redshifts is limited by Galactic hydrogen opacity, and at high redshifts by the intervening intergalactic medium! The detection of $z > 2$ QSOs in the Hamburg quasar survey, which are not only bright but also have a clear line of sight, are ideal to investigate the Lyman limit region. Five of these objects have *HST*/FOS spectroscopy in the ~300 to ~1000 Å wavelength range. There does not seem to be any evidence of a Lyman edge feature in these objects after the spectra have been dereddened, corrected for the individual Lyman limit systems and cumulative H I continuum absorption of Lyα clouds with low column densities. Once again, if we use the Zheng et al. UV composite, the Lyman edge feature is quite narrow (~5%) and is thus not likely to be from a disk. With the *Far-Ultraviolet Spectroscopic Explorer* (*FUSE*) coming on-line, we will have opportunity to investigate the ~450 to ~1200 Å region in the AGN rest frame for a larger sample of objects.

3.3. Polarization

In simple geometrically thin, optically thick accretion disk models, the atmospheric opacities may be dominated by electron-scattering opacity. Also, as we discuss in § 4 below, Compton scattering is often used to alleviate the Lyman edge problem. In a quasi-flattened geometry, the scattering of photons (both Thompson and Compton) leads to polarization of the photons. Thus polarization of the optical/UV continuum in AGNs can also be used as a diagnostic of accretion disk characteristics.

As we noted above at the end of § 2, observations do not confirm the simple electron-scattering–dominated accretion disk predictions for polarization. Observed polarizations are low and are parallel to the inferred disk axis (Stockman et al. 1979, 1984; Antonucci 1988). These observations also found that there was no wavelength dependence of the polarization. Recent optical spectropolarimetry of intermediate and high redshift quasars by Berriman et al. (1990) and Antonucci et al. (1996) confirm the earlier results; i.e., *unobscured AGNs show low optical polarization with no statistically significant wavelength dependence*.

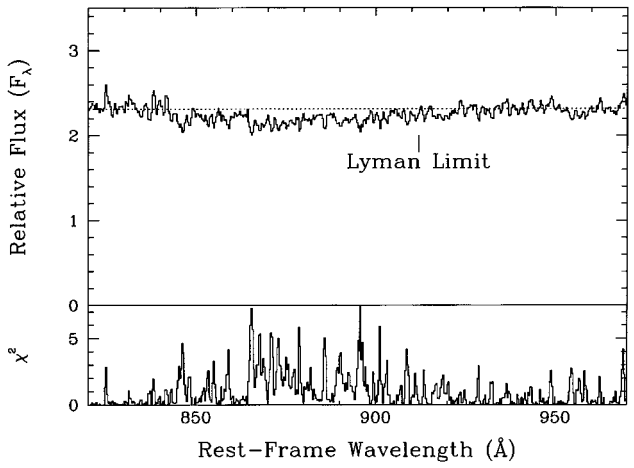

FIG. 8.—Spectral energy distribution in the Lyman limit region for the UV composite generated from *HST*/FOS data. The dotted line represents the continuum fit using the entire *HST* composite. The χ^2 values for each bin relative to the continuum fit are shown in the bottom panel. The ~10% trough seen shortward of the Lyman limit may be indicating that many AGNs have a very weak Lyman edge feature. But given the observational caveats discussed in § 3.1, the presence of this feature cannot be used effectively to quantify the nature of the spectral feature at the Lyman limit (courtesy W. Zheng).

In the unified scheme for AGNs, the accretion disk will not be viewed over the full range of inclination angles because of the obscuring torus. Assuming that the accretion disk axis and the torus axis are aligned, then depending on the opening angle of the torus, the expected polarization range is no longer 0%–11.7% (see § 2) but is reduced. Figure 9 compares the observed polarization of PG QSOs to the predictions for an optically thick, pure electron-scattering slab. In this comparison the viewing angle ranges between 0° and 60°. The comparison shows that the theoretical predictions are inconsistent with the data, i.e., calculations predict more objects with higher polarization than are observed. But, if there is a range in the opening angle of the torus around 30°, then the expected polarization would be in the range 0%–0.5%, which could become consistent with the data. The slightly higher polarization seen in some sources could then be due to larger torus opening angles. Note that in this argument, we have assumed that the disk and torus are aligned, which may not be the case. The important point is that although it may be possible to explain to some extent the low *magnitude* of polarization that is observed in AGNs, the polarization angle is observed to be *parallel* to the inferred disk axis. This polarization angle dependence is perpendicular to that expected from a pure electron-scattering slab! Until recently, the disk axis has been inferred only in radio-loud AGNs by determining the radio jet axis. We now have the

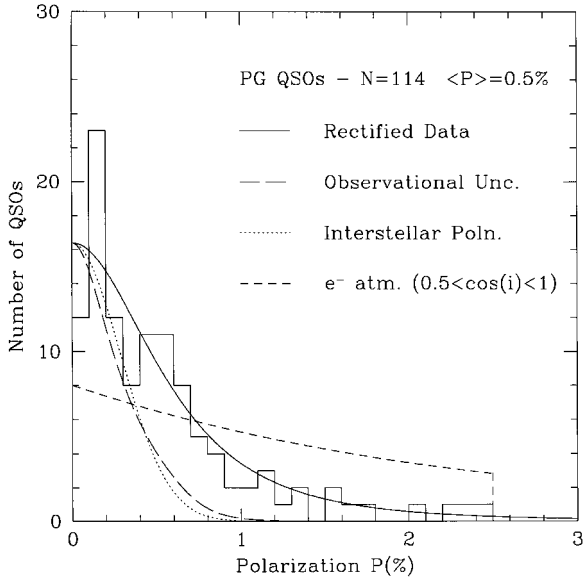

FIG. 9.—Observed optical polarization of PG QSOs compared to predictions (*short-dashed line*) for optically thick, pure electron-scattering slabs with viewing angles in the range of 0°–60° inclination angles. The comparison shows that the theoretical predictions are inconsistent with the data, i.e., calculations predict more objects with higher polarization than are observed. The polarization data are based on the figure by Berriman et al. (1990). The long-dashed line represents the polarization distribution given the observational errors. The dotted line represents the distribution for interstellar polarization only (courtesy E. Agol).

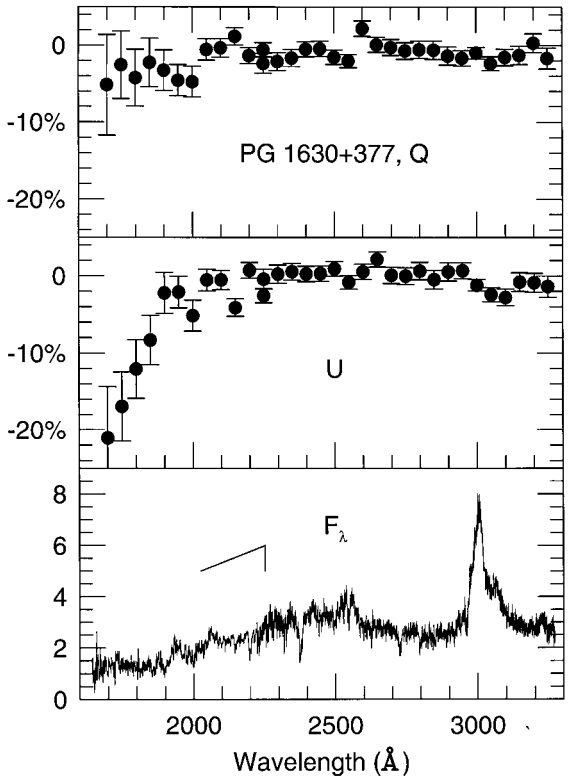

FIG. 10.—*HST*/FOS spectropolarimetry of PG 1630+377 in the Lyman limit region. The normalized Stokes parameters Q/I and U/I are shown in the top two panels. The bottom panel shows the total flux (F_λ) in units of 10^{-15} ergs s^{-1} cm^{-2} $Å^{-1}$. Such a high degree of polarization is rare in radio-quiet AGNs. Approximately 30% of the objects investigated in the Lyman limit region show a rise in polarization shortward of the Lyman edge.

ability to resolve the central radio source in radio-quiet AGNs, and it will certainly be interesting to check the alignment of the polarization angle in these objects.

HST/FOS spectropolarimetry allowed us to probe the ~700 Å to ~1300 Å region of 10 intermediate-redshift quasars (Koratkar et al. 1995; Impey et al. 1995; Koratkar et al. 1998). Using ground-based spectropolarimetry, Antonucci et al. (1996) have observed three high-redshift AGNs shortward of the Lyman limit and 20 intermediate-redshift AGNs in the ~1100 Å to ~3000 Å region. Although the current data cannot be used to make any statistically significant conclusions, there are certain trends seen in this small sample. The data show that polarization is not only low in the optical region but also continues to remain low ($\lesssim$1.5%) even in the UV (up to ~1000 Å). Further, there is no statistical wavelength dependence to the polarization for wavelengths greater than 1000 Å. Investigations shortward of the Lyman limit region found that some radio-quiet AGNs are polarized in this region, and the polarization has some wavelength dependence (see Fig. 10). Approximately 30% of the objects investigated in the Lyman limit region show a rise in polarization shortward of the Lyman edge; i.e., these objects show higher polarizations *shortward of the Lyman edge and no polarization longward of the Lyman edge*. In one case, PG 1630+377, the polarization is ~20%! The other 70% of the sample showed no significant polarization (see Fig. 11). The 95% confidence level upper limits on linear polarization shortward of the Lyman limit for these objects is $\lesssim$4%. It must be noted here that most of the objects that showed polarization shortward of the Lyman limit also showed a candidate partial Lyman edge feature, while except for one object, all the objects that had no detected Lyman edge feature showed no polarization.

3.4. Fe Kα Emission Line and the Lyman Edge

The Fe Kα emission line, interpreted as arising from fluorescence in the X-ray–illuminated disk, is extremely broad and redshifted, which provides dramatic support for an accretion disk in a relativistic potential well (Tanaka et al. 1995). It is perhaps the best evidence for accretion disks in the innermost regions of the central engines of AGNs. It certainly provides the only direct evidence for cold gas with a large column density very close to the central engine. It is therefore important to investigate the nature of the Lyman edge feature in objects that have such convincing evidence of an accretion disk. Unfortunately, there are no observations spanning a reasonable wavelength region (see § 3.2) around the Lyman limit for an AGN that also shows a broad Fe Kα line. The best data come

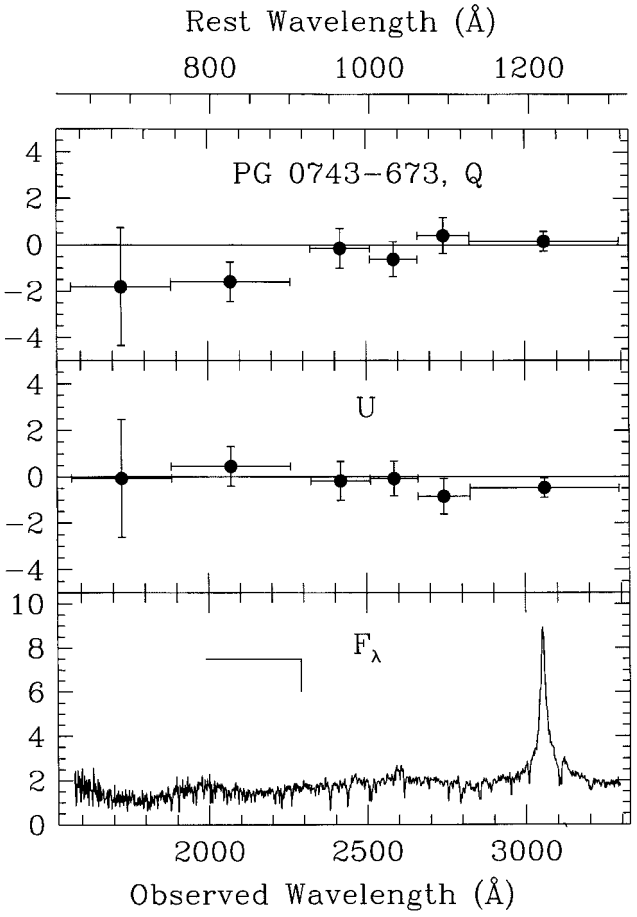

FIG. 11.—*HST*/FOS spectropolarimetry of PG 0743−673 in the Lyman limit region. The normalized Stokes parameters *Q*/*I* and *U*/*I* are shown in the top two panels. The bottom panel shows the total flux (F_λ) in units of 10^{-15} ergs s^{-1} cm^{-2} $Å^{-1}$. Approximately 70% of the sample observed in the Lyman limit showed no significant polarization.

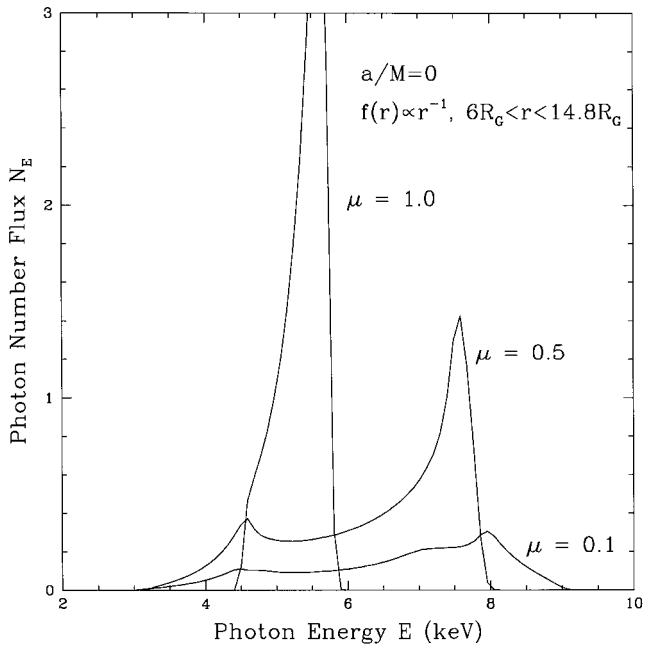

FIG. 12.—Fe Kα line profiles for accretion disks around a Schwarzschild black hole at different inclination angles i ($\mu \equiv \cos i$). The line is assumed to be emitted locally as nearly a delta function in energy at 6.4 keV. A line emissivity profile $f(r)$ which falls off as $1/r$ with radius r has been assumed, extending from the innermost stable orbit to 14.8 R_G. Lines are broader for edge-on disks than for face-on disks. This figure should be compared with Figs. 13 and 19, which show predictions for Lyman edges at similar inclination angles.

from the Hopkins Ultraviolet Telescope (HUT) on low-redshift Seyfert galaxies (Kriss et al. 1997), and *ASCA* observations of these Seyfert galaxies. There are only six Seyfert galaxies that have both Lyman edge and Fe Kα line observations. Except for perhaps one object (NGC 3516), none of the remaining five objects shows a clear intrinsic Lyman edge feature in total flux. Confusion with Galactic absorption in high-n Lyman series lines and the Lyman continuum preclude using the HUT data to search for the smeared edge features expected from a relativistic disk.

Observations of the Fe Kα emission line and the Lyman limit region can be used to constrain the theoretical accretion disk models. The Fe Kα line profiles and line peaks are dependent on the inclination angle of the accretion disk. Although the black hole mass and geometry influence the line profile shape, in general the models predict that the line profiles are broader and the line peaks are bluer for edge-on disks than for face-on disks (see Fig. 12). Therefore, if the line profile is accurately determined, it places strict constraints on the disk inclination angle. Next, if one assumes that the Lyman edge is also from the same disk structure (which need not be the case), then the predicted Lyman edge can be compared with observations (see Figs. 12 and 13). The current Fe Kα emission-line profiles exclude edge-on disks whose Lyman edges are easier to hide owing to large relativistic smearing. The disk inclination angles derived from the Fe Kα emission-line profiles indicate that in a "bare" disk (i.e., no Comptonization), the Lyman edge should be detectable. The current data therefore once again suggest that Comptonization is important.

The Lyman edge problem indicates that to understand the emission mechanism in AGNs, multiwavelength data are essential to constrain the models. With *FUSE* coming on-line, in addition to high-energy resolution X-ray telescopes such as the *X-ray Multi-Mirror Observatory* (*XMM*), there will soon be an opportunity to investigate the Fe Kα emission line and the Lyman edge simultaneously.

3.5. Variability

The extraordinary luminosities of AGNs are observed to vary. Variability studies provide crucial data concerning the timescales of variation, the nature of spectral variation, and the delays between the various spectral regions. Variability data are also essential for understanding the nature of accretion disks

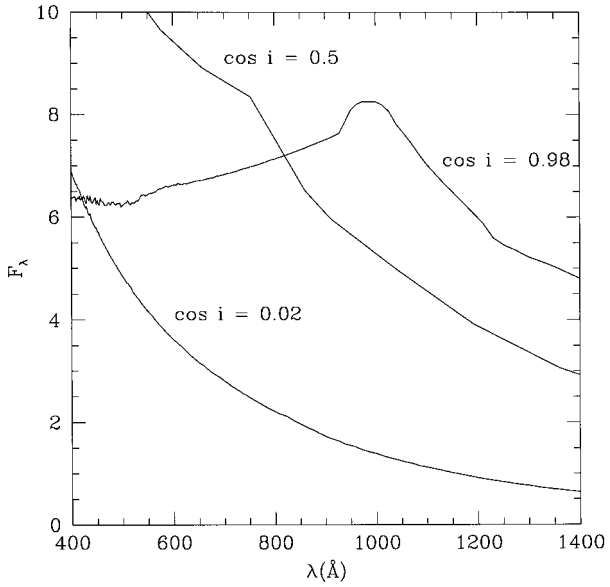

FIG. 13.—Predicted spectral energy distribution in the Lyman limit region for accretion disks around a Schwarzschild black hole at different inclination angles i ($\mu \equiv \cos i$). Spectral features are much more visible for face-on disks ($\cos i = 0.98$) than for edge-on disks. Here the accretion disk is considered to be made of pure hydrogen and helium. Non-LTE effects and relativistics transfer function have been fully incorporated. External illumination of the disk by X-rays has been neglected, which may increase the prominence of the Lyman edges (cf. Fig. 19).

in AGNs because variability timescales allow us to probe the nuclear regions ($<10^{14}$–10^{18} cm). If characteristic timescales are found, these would allow us to investigate the physical mechanisms that drive the fluctuations. By comparing multi–waveband light curves, the nature of propagation of a signal can be investigated.

3.5.1. Variability Timescales

Variability timescales range from hours to years depending on the luminosity of the AGN, and the observed wavelength range. The most commonly observed X-ray variations in Seyfert galaxies are about a few hours (Green, MacHardy, & Lehto 1993; Nandra et al. 1997a). The shortest timescale variation in the optical/UV observed so far is ~2 days for NGC 4151 (Crenshaw et al. 1996). Although ultrarapid variations are seen in the X-rays, there is as yet no detection of ultrarapid variability (i.e., variations on timescales of hours) in the optical and UV (Welsh et al. 1998). On average, the optical/UV continuum in Seyfert galaxies and lower luminosity quasars varies over timescales of weeks to months (Kaspi et al. 1996; Givon et al. 1998). The monitoring campaigns so far have found no convincing evidence for any characteristic timescales or periodicities (see, e.g., Netzer & Peterson 1997; Ulrich, Maraschi, & Urry 1996; Mushotzky, Done, & Pounds 1993 for excellent reviews).

3.5.2. Spectral Variations in the Optical/UV/X-Rays

The nature of the spectral variations allows us to characterize the emission mechanism and the factors that cause changes in the emission mechanism. Spectral variations are such that the optical/UV continuum hardens as the nucleus brightens (see Fig. 14). The shortest wavelengths vary the fastest (Clavel et al. 1992; Edelson et al. 1996; Peterson 1993; Nandra et al. 1998). In the X-rays, the power-law component often varies with no spectral variation (Ulrich et al. 1996; Nandra et al. 1998), but sometimes the spectrum does change, becoming softer as the object brightens (e.g., 3C 390.3, Leighly et al. 1997; NGC 5548, Magdziarz et al. 1998). Increased Compton cooling of the X-ray–emitting plasma, possibly because of a change in the disk geometry producing more UV photons (see Magdziarz et al. 1998; see § 5 below), may be an explanation for this. We discuss the implications of spectral variations further in § 4 below.

3.5.3. Correlations between the Optical/UV and X-Rays

One of the main characteristics of optically thick accretion disks is that different portions of the optical/UV spectrum arise predominately from spatially separated locations in the flow that have different overall size scales. Variability in the continuum might therefore have wavelength-dependent timescales and amplitudes, and one might also expect time lags owing to finite signal propagation speeds between different regions of the flow. For quite some time now, it has been known that variations in the optical/UV continuum of Seyfert galaxies and QSOs are highly correlated and imply signal propagations on faster timescales than the viscous or even sound-crossing times in the flow (Alloin et al. 1985; Cutri et al. 1985; Courvoisier & Clavel 1991). One possible explanation for this is that optical/UV variations are driven by reprocessing of UV or X-ray radiation from the inner parts of the disk (Krolik et al. 1991; Collin-Souffrin 1991). This is confirmed by simultaneous, multiwavelength monitoring campaigns of the Seyfert galaxies NGC 4151 and NGC 5548, which show correlated variability between optical/UV and X-ray energies (Edelson et al. 1996; Clavel et al. 1992).

NGC 7469 has been intensively monitored for the longest duration so far, and this campaign allowed time lags between the different continuum wave bands to be measured for the first time. In this source, optical/UV continuum variability is highly correlated and shows a monotonically increasing time lag τ with wavelength λ, which can be fitted with $\tau \propto \lambda^{4/3}$, the prediction for a $T_{\rm eff} \propto r^{-3/4}$ accretion disk (Wanders et al. 1997; Collier et al. 1998). The time delays ranged from $\simeq$0.2 to 2 days, and their statistical significance is difficult to determine. A conservative analysis by Peterson et al. (1998) finds them to be marginally significant ($>2.2\ \sigma$). Peterson et al. (1998) also showed that if the results for NGC 7469 are real and if we scale all the other AGNs with previous observations, the data from previous campaigns did not have the temporal resolution to detect lags if they were present.

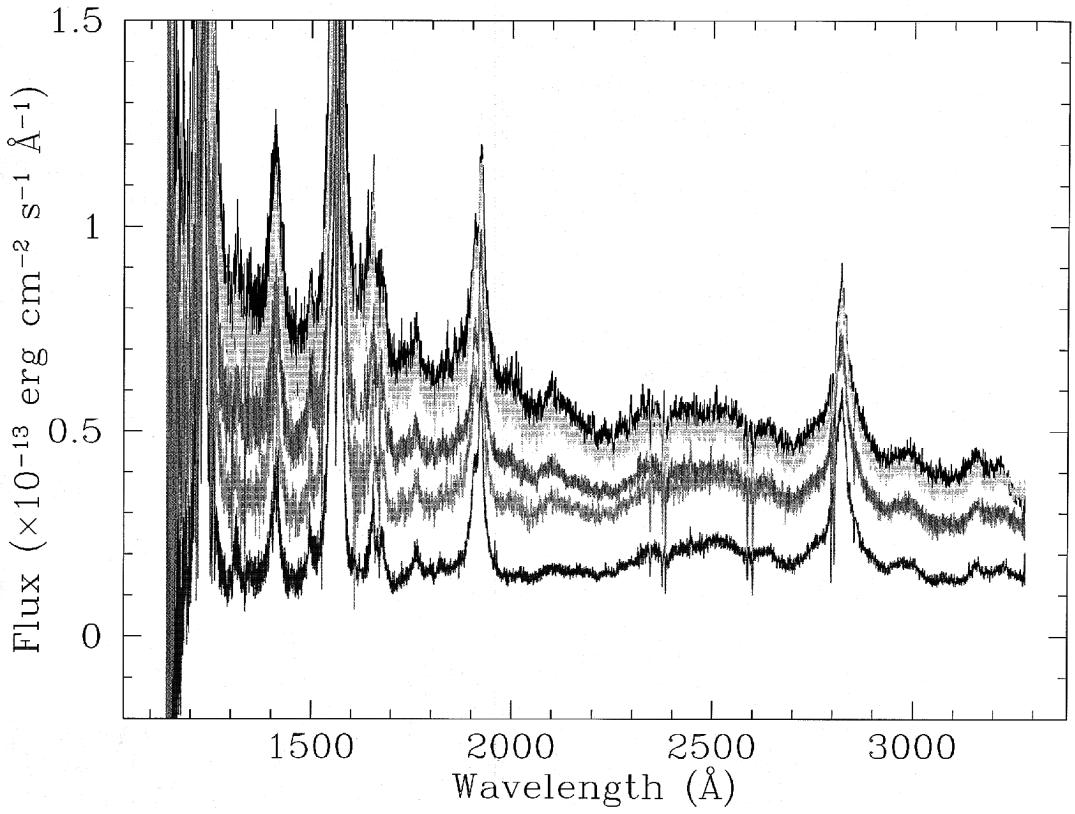

FIG. 14.—*HST*/FOS observations of NGC 3516. The observations were obtained over a period of a year and show a factor ~ 5 variation at 1360 Å and a factor of ~2 variation at 2200 Å. This type of variation, where the shortest wavelengths vary more than the longer wavelengths, is typical of AGNs. Thus the optical/UV continuum hardens as the nucleus brightens.

More interestingly, variability in the X-rays and optical/UV is *not* correlated on such short timescales (Nandra et al. 1998). However, one can interpret the data in terms of an *anticorrelation* between the X-rays and UV, with the X-rays leading the UV by 4 days. Alternatively, the UV correlates with the X-rays, with the UV leading by 4 days. Neither of these statements provides a satisfactory representation of the light curves, which appear to show the UV leading the X-rays near the peak fluxes, while they both achieve approximate simultaneity near the minimum flux levels (see Fig. 15). The X-rays also show short timescale variability (50% in 1 day), which is not observed in the UV. While this last fact is consistent with the optical/UV radiation arising on larger scales from reprocessing of X-rays from the inner disk, the lack of short timescale correlations presents a severe problem for this simple picture. Models in which the UV drive the X-rays by providing the seed photons for Compton scattering are also too simple to explain the observations. As Nandra et al. (1998) point out, the observations require a more complex interaction between the UV- and X-ray–emitting regions. One possibility that they propose is that in bright states the source of UV seed photons lies 4 lt-days out from the X-ray source and drives the X-ray variability. This source of seed photons is lost in faint states, where closer sources of seed photons become important. It is not yet clear how to reconcile the UV/X-ray variations with a flow geometry.

Another indication from the NGC 7469 campaign that things are not so simple is the fact that, while the broad emission lines do tend to show correlated, lagged variability with the observed UV continuum, in this particular campaign they also showed long-term trends that were *not* present in the continuum, which suggests that either the observed UV photons are not in fact a good representation of the variability in the (unobservable) ionizing photon spectrum or that the broad line region is evolving over this period.

3.6. Microlensing

As we noted in the Introduction, direct imaging of the central accretion flow will be impossible for the foreseeable future because of the small size scales involved. Reverberation mapping in the X-rays may provide one way of probing the accretion flow with the next generation of high-throughput X-ray satellites such as *XMM* and *Constellation-X*. In addition,

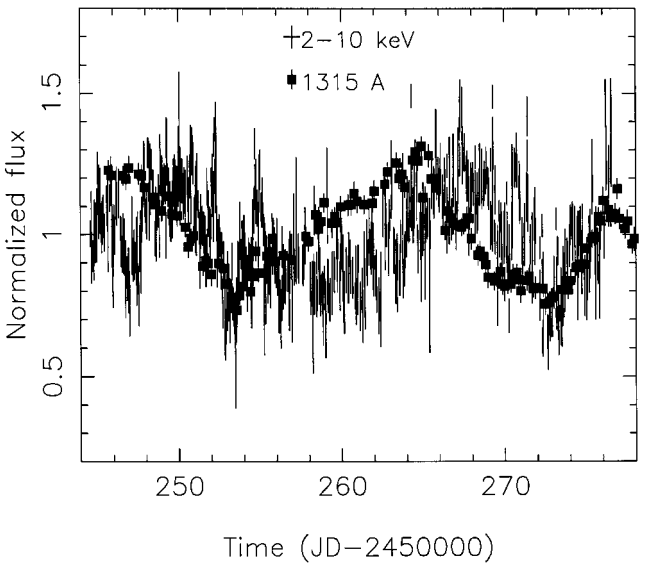

FIG. 15.—X-ray and UV variability for NGC 7469. The UV variations are leading the X-rays near the peak fluxes, while they both achieve approximate simultaneity near the minimum flux levels. The X-rays also show short timescale variability (50% in 1 day), which is not observed in the UV. These observations indicate that there is complex interaction between the UV- and X-ray–emitting regions, and it is not clear how to reconcile the UV/X-ray variations with a flow geometry (courtesy K. Nandra).

Nature has provided us with a cosmic telescope that can optically perform this feat, at least in one source. The line of sight to quasar Q2237+0305 passes right through the central core of a foreground, face-on spiral galaxy. This galaxy lenses the quasar into four images that make up the "Einstein Cross" (Huchra et al. 1985). Because of the large surface density of stars in the galaxy's central region, microlensing is observed in the images (Irwin et al. 1989; Pettersen 1990; Corrigan et al. 1991; Racine 1991; Nadeau et al. 1991; Racine 1992; Østensen et al. 1996). The size of microlensing variations implies that the quasar emission region must be smaller than the scale of variations in the caustic network formed by the foreground stars. This scale is typically given by the Einstein radius $\sim 10^{17} M^{1/2}$ cm, where M is the mass of the lensing star in solar masses. If a rapid microlensing event is resolved in time, even more stringent constraints can be placed on the source size. The most rapid observed event in image "A" (Irwin et al. 1989) constrains the size of the optical emission region to be $\leqslant 2 \times 10^{15}$ cm (Wambsganss, Schneider, & Paczyński 1990). This is far below any length scale that can be probed by other techniques.

The small size of the optical emission region places strong constraints on accretion disk models. Rauch & Blandford (1991) found that to explain both the observed luminosity and the microlensing size scale, an emissivity in excess of the blackbody limit was required. In other words, a thermal accretion disk is too large (by about a factor 3) to fit within the microlensing size constraint. Somewhat different modeling by Jaroszyński, Wambsganss, & Paczyński (1992) found that accretion disks were consistent with the microlensing constraint. Part of the difference between these two papers was that Jaroszyński et al. considered accretion disks around Kerr holes, whereas Rauch & Blandford considered only Schwarzschild holes. This allowed the former authors to consider more compact disks, as well as producing a greater concentration of luminosity in a hot spot produced by beaming of radiation toward the observer by the orbiting emitting plasma.

However, an even more important difference between the two papers is how the SED problem was handled. As we have pointed out here in this review, luminous accretion disks produce SEDs that are too blue compared to observations. To get around this, Rauch & Blandford modified the radial emissivity of the disk to be flatter than equation (1) above, i.e., allowing more of the accretion power to be dissipated at larger radii. This is one way of explaining the red observed SEDs of AGNs but of course leads to larger optically emitting regions than the standard disk. Jaroszyński et al., on the other hand, kept the standard radial emissivity and assumed instead that there was another source of red light in the source that arises from farther out and is not microlensed. Both approaches are ad hoc, although there are other reasons for believing that the radial emissivity profile that Rauch & Blandford assume is correct: optical/UV variability suggests that it arises from reprocessing of radiation from the inner disk. Czerny, Jaroszyński, & Czerny (1994) have explored the problem of irradiated disks and again find accretion disks to be consistent with the microlensing data. However, they found it necessary to consider accretion luminosities half that of Eddington, so a slim disk (see § 5.2 below) really needs to be considered. The microlensing problem is clearly intimately tied to the SED problem, and continued monitoring is crucial to tighten the observational constraints.

While the microlensing observations have often been presented as a challenge for accretion disk models, it is perhaps worthwhile pointing out that they do in fact prove that the optical emission in at least this quasar originates very close to the central black hole. This is at least in qualitative agreement with the idea that the central accretion flow is responsible for the BBB.

3.7. Double-peaked Line Profiles

Broad emission lines are characteristic of the spectra of AGNs. If these lines arise in a disk, one expects them to exhibit the double-peaked profile structure that is commonly seen in the optical/UV emission lines from accretion disks in cataclysmic variables (see, e.g., Marsh & Horne 1988). Yet, only a fraction of radio-loud AGNs, and a handful of radio-quiet AGNs, show such lines (Eracleous & Halpern 1994; Storchi-Bergmann et al. 1997). This has been raised as a problem for accretion disk models of AGNs (Kinney 1994). However, it is

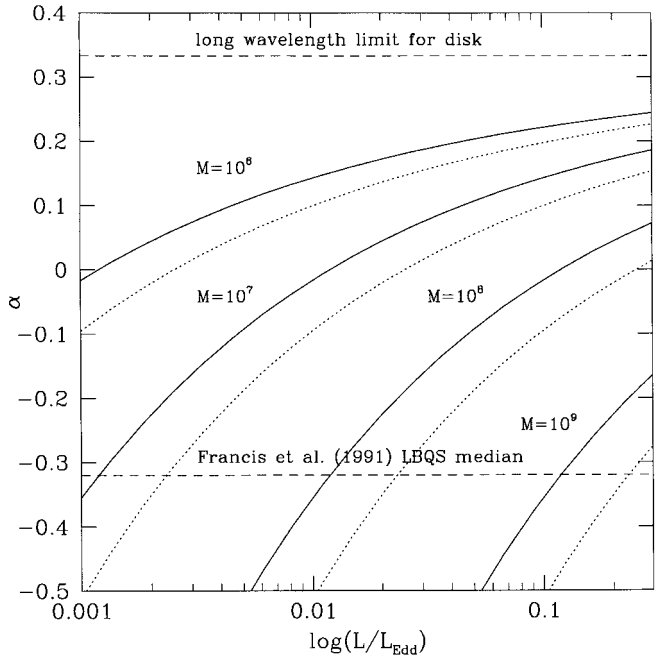

FIG. 16.—Optical/UV slopes predicted by simple blackbody accretion disk models around Schwarzschild black holes, as a function of luminosity. The relativistic transfer function has been included here, with the upper (*solid*) and lower (*dotted*) of each pair of curves corresponding to inclination angles of 66° and 26°, respectively. (The former are close to what one obtains when neglecting the transfer function.) The slopes are calculated between 1450 and 5050 Å. These predicted slopes are significantly redder than the $\nu^{1/3}$ long wavelength limit. The mean continuum slope determined by Francis et al. (1991) can be generated by a range of disk parameters. (For blackbody disks, the shape of the spectrum depends only on $L/L_{\rm Edd}/M$, and all the curves for a given inclination angle lie on top of each other when plotted against this parameter.)

also worth noting that Livio & Xu (1997) have shown that the double-peaked lines cannot be produced by two line-emitting jets, thus leaving the accretion disk as the only viable site for the production of such lines.

In accretion disk models the optical/UV continuum is generated from disks whose extent is 10–1000R_g. If the optical/UV continuum is generated by an accretion disk, it is tempting also to hypothesize that the broad emission line spectrum is due to the disk. Collin-Souffrin (1987) showed that if a disk is illuminated by an external X-ray source, then the disk could contribute toward the emission-line spectrum, but the emission lines were from the outer parts of the disk at ~1000R_g, and broad emission lines were not observed from the inner parts of the disk (Dumont & Collin-Souffrin 1990a, 1990b). Models by Chen, Halpern, & Filippenko (1989) and Chen & Halpern (1989) also effectively illuminate the outer parts of the disk to produce the low-ionization lines (Mg II and Balmer lines). In all the models, although the emission lines may be related to the disk phenomenon, the lines are formed at relatively large distances from the massive black hole, and we are interested in the inner parts of the accretion disk that predominantly contribute to the optical/UV continuum. Therefore in this paper we do not discuss broad emission line profiles further. Ultimately, the ionizing continuum that is generated by the inner disk drives the emission lines, and in a realistic model both the lines as well as the continuum will have to be explained. For a review on emission-line profiles from disks, we refer the reader to Eracleous (1998).

Before leaving this subject entirely, it is perhaps worthwhile pointing out that the Fe Kα line observed by *ASCA* in many Seyfert galaxies does occasionally have a double-peaked shape (see, e.g., Tanaka et al. 1995). We have discussed the Fe Kα line in § 3.4 since this line is expected to arise within 100R_g.

4. MORE RECENT ACCRETION DISK MODELS

4.1. The Big Blue Bump

Since the SED predicted by luminous accretion disks is generally bluer than the optical spectra observed in AGNs, traditionally theoretical fits to the data included an additional infrared power-law component that changed the optical slope that the accretion disk model had to fit. But, with mounting evidence that thermal dust emission produces the infrared, this ad hoc procedure is not valid, and such disk models do not provide a satisfactory fit to the observations. Driven by the challenges posed by observations to the standard model, much more sophisticated modeling of accretion disks has occurred in recent years.

Before turning to these more sophisticated models, it is important to be clear as to what the elementary blackbody disk models can and cannot do. Naively, one would expect these simple models to predict that the SED should be $F_\nu \propto \nu^{1/3}$. However, the simplest thin disk models around supermassive ($M \geq 10^6\ M_\odot$) black holes often *do not* produce $\nu^{1/3}$ spectra throughout the optical/UV. In order for the disk not to produce so much radiation pressure that it becomes geometrically thick, the accretion rate is limited to about 0.2–0.3 times the Eddington rate (see, e.g., Laor & Netzer 1989, but see § 5.2 below). Simple blackbody disk models around supermassive black holes have maximum temperatures less than 3–8 × 10^5 K, depending on the black hole spin, and their SED in the optical/UV can be significantly redder than the $\nu^{1/3}$ prediction (see Fig. 16), particularly when viewed face-on.

A fit to the Francis et al. (1991) composite spectrum is shown in Figure 17. There is no problem fitting the data with a simple blackbody disk model, provided the disk is *cool*. The Schwarzschild fit shown in this figure has $L/L_{\rm Edd} \simeq 0.1(M/10^9\ M_\odot)$, whereas the Kerr fit has $L/L_{\rm Edd} \simeq 3 \times 10^{-3}\,(M/10^9)$. Such cool disk spectra turn over in the optical/UV, which is why they can have such red slopes. This curvature in the disk spectrum immediately provides an explanation for why the optical/UV continuum might get harder when brighter: varying the maximum temperature, e.g., by varying the accretion rate, will change the overall slope of the

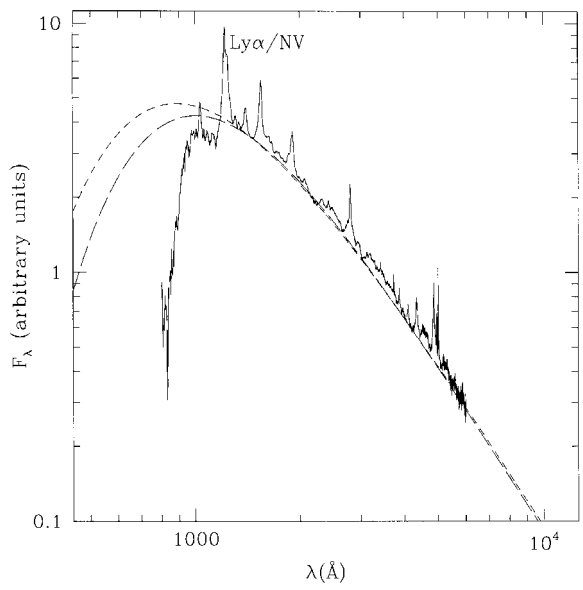

FIG. 17.—Best-fit blackbody accretion disk spectra to the line-free continuum windows of the composite quasar spectrum of Francis et al. (1991). The solid curve shows the composite spectrum; the short-dashed curve, a disk model around a Schwarzschild hole; and the long-dashed curve, a disk model around a Kerr hole with $a = 0.98M$. The relativistic transfer function has not been included in these fits. Note that the data in the composite spectrum shortward of the Lyα/N v line is contaminated by intervening absorption in the intergalactic medium.

spectrum (Collin-Souffrin 1991; Molendi, Maraschi, & Stella 1992). However, such cool disks are probably not sufficiently luminous, at least if they are around low-mass black holes, and they certainly do not produce much in the way of ionizing photons! One possibility may be that the optically thick portion of the disk does not extend all the way to the innermost stable orbit, which allows it to have a smaller maximum temperature as the flow transitions into some other, hotter phase (see, e.g., § 5.5 below).

The more difficult continuum SED problem with thin disk models is not how to explain a red optical/UV spectrum but rather how to explain the origin of the higher energy EUV/X-ray emission. In Figure 17 we see how the theoretical continuum SED falls off sharply in the EUV. This problem is highlighted when one tries to understand the AGN emission-line spectrum. For example, since the BBB drives the emission lines seen in the spectra of AGNs, Korista, Ferland, & Baldwin (1997) compared the predicted and observed emission-line strengths using the "observed" UV X-ray composite BBB SED (see § 3.1) in photoionization models. The "observed" BBB SED does not reproduce the observed line strengths. MacAlpine et al. (1985) first showed that the He II line equivalent widths were indicative of substantial intrinsic UV excess seen by the broad-line clouds. To explain the discrepancies between the "observed" BBB and the theoretical predictions, we either have to assume that the observations are invalid or that the BLR clouds see a very different continuum than that observed by us. This exercise clearly indicates that geometry of the gas near the AGN central engine and/or the presence of another emission component that generates a significant amount of the ionizing radiation must also be considered.

If the accretion disk itself is to be hot enough to produce sufficient ionizing continuum, then the optical SED predicted by simple blackbody models will indeed be too blue to explain the observations. The accretion disk is not likely to emit locally as a blackbody, however. As noted in § 2, for example, electron scattering can significantly flatten the spectrum in frequency (i.e., make it redder) if it dominates the opacity at the photosphere and produces a modified blackbody spectrum. Whether or not this happens depends on the very uncertain vertical structure of the disk. Laor & Netzer (1989) were the first to make a serious attempt at improving the simple models by calculating the vertical structure and radiative transfer in an approximate fashion, including bound-free as well as free-free and electron-scattering opacities. They found that the photosphere temperature is everywhere close to the effective temperature for most of their AGN disk models, which indicates that a blackbody spectrum is a better local approximation than a modified blackbody. However, this conclusion is uncertain, as it depends crucially on the density at the photosphere that in their models was equal to the midplane density. This may have artificially enhanced the role of absorption opacity to scattering opacity at the photosphere. Ross, Fabian, & Mineshige (1992) improved on the Laor & Netzer models by again assuming a constant density with height but including a better treatment of Comptonization in both the radiative transfer and thermal balance. They found that the overall spectrum did deviate significantly from the blackbody assumption, at least for their chosen viscosity. More detailed treatments of the vertical structure in such models, but that *neglect* bound-free and bound-bound opacities, have been performed by Shimura & Takahara (1993, 1995) and Dörrer et al. (1996).

One way of redistributing the energy in the BBB and changing the optical/UV continuum slope is to assume that the optical/UV arises from reprocessing of radiation from the inner disk. A flat disk irradiated by a central source still produces an $r^{-3/4}$ temperature profile, so flaring or warping is required to change the spectral shape (see § 5.4). Until recently, the reprocessing assumption was valid because the variability campaigns indicated that the optical/UV and X-ray variations were correlated with nearly no lag. However, the NGC 7469 campaign raises a number of issues that make this simple picture of reprocessing even more complicated (see § 3.5.3).

4.2. The Lyman Edge

To explain the dearth of Lyman edges in AGNs, the new accretion disk models have considered a number of theoretical approaches and improvements. The new models now include complex stellar atmosphere effects, and modern state-of-the-

art stellar atmosphere codes. Preliminary steps have been taken toward investigating two-phase accretion disk models and including relativistic transfer functions in the codes.

The original calculations of accretion disks by Kolykhalov & Sunyaev (1984) relied on existing stellar atmosphere libraries and thus predicted large Lyman edge features. These libraries completely neglected non-LTE effects. These can be very important in the Lyman limit region because the large hydrogen photoionization opacity generally means that the Lyman continuum originates high in the atmosphere, where densities are low and radiative transition rates can dominate collisional transition rates. Even more important, the atmospheres that exist in those libraries generally have high densities compared to what is possible in high-luminosity accretion disks. This limited the range of parameter space that Kolykhalov & Sunyaev could explore to low-α parameter ($\alpha < 10^{-2}$), high photospheric density models. Because the neutral fraction of hydrogen becomes larger at high densities, this resulted in very large Lyman edge absorption opacity, thereby producing very large absorption edges in these disk models.

Low densities in the disk photosphere will reduce the ratio of Lyman continuum absorption opacity to scattering opacity and thereby decrease the flux difference at an absorption edge or even drive it into emission (Czerny & Pojmański 1990). Ab initio radiative transfer calculations confirm this behavior (Coleman & Shields 1993; Shields & Coleman 1994; Hubeny & Hubeny 1997; Sincell & Krolik 1998), which shows that as the maximum effective temperature and/or the ratio of luminosity to Eddington luminosity increase, Lyman absorption edges become weaker, then disappear, become moderate emission edges, and finally become weak emission edges as the hydrogen becomes fully ionized and recombination rates are low. Non-LTE effects produce similar results (Sun & Malkan 1989; Shields & Coleman 1994; Störzer, Hauschildt, & Allard 1994; Hubeny & Hubeny 1997; Collin & Dumont 1997; Czerny & Dumont 1998). Ironically, non-LTE effects can also *enhance* the He II Lyman continuum (Hubeny & Hubeny 1997), which would have important implications for photoionization of the broad-line region clouds in AGNs. To get rid of the Lyman edge completely in a given atmosphere at a given radius in the disk using these effects would require fine tuning, but it is clear that the overall edge produced from an integration of diverse atmospheres at different disk radii, some with absorption edges and some with emission edges, might generically produce a small net effect (see Fig. 18). Note, however, that the requirement that the disk be hot enough to drive the edge into emission in the innermost radii requires high accretion rates compared to Eddington, which drives the optical/UV SED closer to the classic $F_\nu \propto \nu^{1/3}$ limit (Sincell & Krolik 1998). The relatively cool disks discussed in the previous subsection to explain the SED would probably have observable Lyman absorption edges (see Fig. 22). There is as yet no accretion disk model that solves both problems (the Lyman edge and the optical/UV continuum slope) simultaneously.

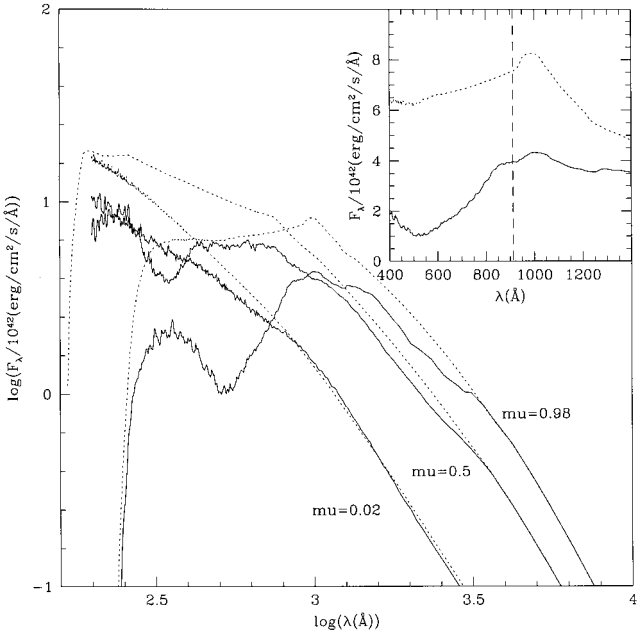

FIG. 18.—Predicted SED of the accretion disk model of Fig. 20, after folding through the relativistic transfer function for three different observer inclination angles i ($\mu \equiv \cos i$). Dashed curves show the non-LTE hydrogen/helium spectra, while solid curves show the spectra as modified by LTE metal line emission and absorption but neglecting metals in the atmosphere structure calculation. The Lyman edge is virtually undetectable except for the near face-on model ($\mu = 0.98$), which for clarity is blown up on a linear scale in the inset. Here the Lyman limit is shown by a vertical dashed line. In this model, a change in continuum slope in the Lyman limit region is still evident for a substantial parameter space (courtesy E. Agol).

To explain the X-ray spectra observed in AGNs, a number of models invoke thermal Comptonization of optical/UV photons by an energetically powerful, magnetized corona above the disk (see, e.g., Haardt & Maraschi 1991). Strong support for such models has been provided by the observation of Compton reflection features in hard X-rays (Nandra & Pounds 1994), which require that cold matter (presumably the disk) cover approximately half of the sky as seen from the X-ray source. Until recently, most accretion disk model calculations explored the parameter space for a "bare" accretion disk and neglected the effects of external heating of the disk atmosphere. Sincell & Krolik (1997) have taken the first steps in calculating the spectrum from an X-ray–illuminated accretion disk. In their simple two-phase model, *all* the accretion power is assumed to be dissipated in a corona above the disk. X-rays from the corona irradiate the accretion disk and the UV continuum is produced by reradiation of absorbed energy. There is no internal disk heating. Their calculations showed large Lyman edge features in emission, which are not present in the observations. Figure 19 shows the emission edges produced for three observer viewing angles by the Sincell & Krolik (1997) models. The sharpest edges occur for face-on disks, but substantial

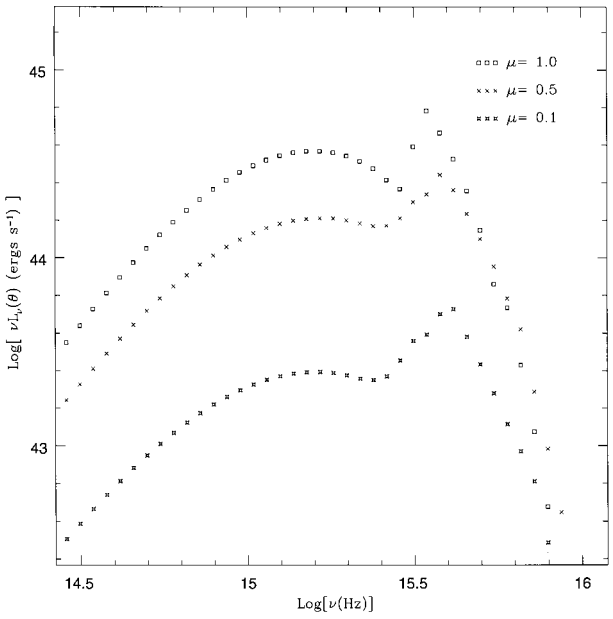

FIG. 19.—Predicted spectra for X-ray irradiated accretion disk with accretion luminosity equal to 3% of Eddington, around a nonrotating black hole of mass $2.7 \times 10^8\ M_\odot$. Each of the three sets of points corresponds to a different observer inclination angle i, where $\mu \equiv \cos i$. The top set of points is more face-on, while the bottom set is more edge-on. The large Lyman edges predicted by these models are not observed (courtesy M. Sincell).

edges are still produced for edge-on disks. Physically, these large emission edges arise because taking accretion power out of the disk and putting it in the corona robs the disk of pressure support, producing larger photospheric densities and therefore larger hydrogen recombination rates. Although the simple two-phase model disagrees with the observations in the Lyman limit region, the parameter space for this model has not been thoroughly examined, and many sophisticated radiative transfer effects, particularly non-LTE effects on the level populations of the irradiated hydrogen gas, have not been included.

The accretion disk is embedded in the deep potential well of the supermassive black hole. It is then natural that many authors have considered the effects of relativistic Doppler shifts and gravitational redshifts to explain the dearth of Lyman edge features in AGNs (Sun & Malkan 1989; Laor & Netzer 1989; Lee, Kriss, & Davidsen 1992; Laor 1992; Shields & Coleman 1994; Wehrse 1997). The amount of Lyman edge smearing is inclination angle–dependent, with the largest effect seen when the object is viewed edge-on. In the unified schemes for AGNs, the objects for which we have observational data (Seyfert 1 galaxies and QSOs) are most likely to be viewed face-on, where the effect of smearing is predicted to be the smallest. The smearing also depends on the black hole spin. Kerr holes are more effective than Schwarzschild holes because the innermost stable orbit can be much closer to the horizon. However, to test effectively the accretion disk models that include all these effects is nearly impossible. Ideally, the observations need to be of an AGN with a "reasonably clean" line of sight and over a large wavelength region, and, as discussed in § 3.2, such observations are rare!

One of the many ways to account for the few observed Lyman edge features in AGNs is to invoke a Compton scattering atmosphere (Czerny & Zbyszewska 1991; Lee et al. 1992). In these models, the spectral shape in the Lyman limit region is a function of the electron temperature of the Comptonizing corona, the optical depth to Compton scattering, and the inclination angle of the accretion disk. The Lyman edge is smeared out because Lyman limit photons are scattered across the Lyman edge, which makes the Lyman limit feature more difficult to detect. The models predict a definite break in the shape of the continuum at the Lyman limit (Lee et al. 1992). This is qualitatively similar to observations of the few candidate "partial" Lyman edge objects. As discussed in the next section, Compton scattering may impart polarization to the radiation higher than observed, but if the corona is magnetized, Faraday rotation can alleviate this problem.

Metal line opacity is likely to be important in the Lyman limit region, and no models exist as yet that properly take this into account. Hubeny & Hubeny (1998) have included this in a preliminary way by including the line opacity and emissivity in radiative transfer calculations through atmospheres whose structure was calculated by *neglecting* these lines. While not fully self-consistent, the results suggest rather strongly that the Lyman edge will be swamped by metal line features (see Fig. 20). Figure 18 shows the corresponding total spectra after integrating over all disk radii and folding through the relativistic transfer function (Agol, Hubeny, & Blaes 1998b). Even in the pure hydrogen/helium models, the Lyman edge is greatly reduced. A change in slope is still evident in the $\mu = 0.5$ case, although it occurs shortward of 912 Å. A bump is present redward of 912 Å in the near face-on case. This is produced because the Lyman edge is in emission in the (more redshifted) inner parts of the disk and in absorption in the (less redshifted) outer parts of the disk (see Fig. 20). When metal lines are included, the change in slope near this bump is reduced but is still detectable conceivably. In addition, the dramatic reduction in flux shortward of 850 Å caused by the line-blanketing in this model could be detected. However, this is the face-on case in which relativistic smearing is most reduced. Self-consistent calculations need to be performed to make firmer predictions, but this work is encouraging.

At long wavelengths the spectra shown in Figure 18 obey $F_\lambda \propto \lambda^{-7/3}$, in agreement with the standard $F_\nu \propto \nu^{1/3}$ accretion disk prediction. However, flux is lost by the line-blanketing effects of metals, which causes the SED to drop at short wavelengths. In a self-consistent calculation, this absorbed radiation will have to be reemitted somewhere in the SED, and it is therefore conceivable that the overall SED continuum shape will change, likely becoming redder and therefore in better agreement with observations. Once again, this needs to be

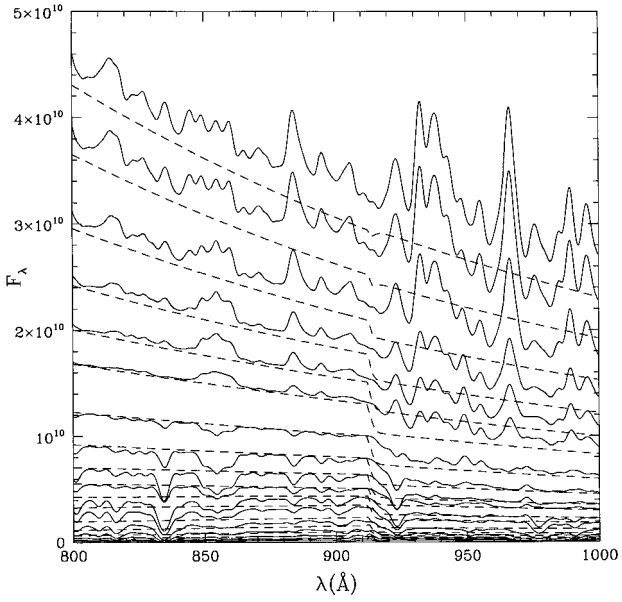

FIG. 20.—Predicted flux emerging locally from various annuli at different radii in an accretion disk model around a Kerr hole of mass $2 \times 10^9\ M_\odot$ and spin $a/M = 0.998$. The accretion rate through the disk is $1\ M_\odot\ \mathrm{yr}^{-1}$. Only the wavelength range near the Lyman limit is shown. Solid curves show the full spectra, including a metal line source function in LTE, but with a fixed atmosphere structure calculated by neglecting metals. The solid curves are therefore not self-consistent but rather indicate that metal lines are likely to be important. Dashed curves show the self-consistent non-LTE continuum spectra computed by neglecting metals (data courtesy I. Hubeny).

checked by computing self-consistent line-blanketed, non-LTE models in a broad range of parameter space.

An important fact about all the new "bare" accretion disk calculations is that *the strength of the Lyman edge feature is not as strong as thought in the earlier models, but getting rid of the Lyman edge is difficult.* Self-consistent calculations of Lyman edge features in disk-corona or multiphase accretion flow models are badly needed.

4.3. Polarization

The Chandrasekhar (1960) calculation of polarization emerging from pure electron-scattering atmospheres is unlikely to apply to real accretion disk atmospheres, which have nonzero absorption opacity. Laor, Netzer, & Piran (1990) made the first attempt at calculating the effects of absorption opacity on the disk polarization of AGNs. They did this by simply multiplying the Chandrasekhar polarization by the ratio of Thomson opacity to total opacity,

$$q(\nu) = \frac{\kappa_{\rm es}}{\kappa_{\rm es} + \kappa_{\rm ab}(\nu)}, \tag{2}$$

which they took to be independent of depth at each radius in the disk. Because $q < 1$ at all frequencies ν by definition, this gives the physically reasonable result that absorption opacity always reduces polarization. The total disk polarization was therefore reduced in their calculations, which therefore produced better agreement with observations. Once again we note, however, that their models may have had high photospheric densities and therefore *might* have exaggerated the importance of absorption opacity compared to scattering opacity. In general they predicted that the polarization should rise with decreasing wavelength up to around the Lyman edge, then drop because of the increase in bound-free opacity, and then rise again. Laor et al. (1990) also included the effects of the relativistic transfer function on polarization and found that at very short wavelengths the plane of polarization rotates away from being parallel to the disk plane.

The effects of absorption opacity on polarization can actually be more subtle than assumed by Laor et al. (1990). Polarization emerging from an atmosphere depends on both the presence of scattering opacity and the degree of anisotropy of the radiation field (limb-darkening or limb-brightening). While absorption opacity reduces the importance of scattering, it can also enhance the anisotropy, depending on the thermal source function gradient. This can sometimes lead to an *increase* in polarization over and above that expected for a pure electron-scattering atmosphere (Harrington 1969; Loskutov & Sobolev 1979; Bochkarev, Karitskaya, & Sakhibullin 1985). The effect is illustrated in Figure 21, which shows polarization as a function of q for thermal source functions that vary linearly with total optical depth τ in the atmosphere:

$$S(\tau) = S(0)(1 + \beta\tau), \tag{3}$$

where the constant β determines the steepness of the thermal source function gradient. As shown in the figure, inclusion of absorption opacity (q dropping below unity) can produce an increase in polarization if the thermal source function gradient is steep. In addition, *flat* thermal source function gradients can produce strong *negative* polarizations, in which the polarization is perpendicular to the disk plane (the "Nagirner effect"). The Nagirner effect might be one way of reconciling the fact that the polarization observed in AGNs is parallel to the radio axes and perpendicular to the Chandrasekhar (1960) prediction. However, it may be difficult for it to produce an optical polarization which is wavelength independent, as observed.

Blaes & Agol (1996) attempted to use these atmosphere effects to explain the steep rises in polarization observed blueward of the Lyman edges in some quasars, discussed above in § 3.3. A good qualitative fit was obtained to the data for PG 1222+228 (Impey et al. 1995) by invoking a relatively cool disk whose overall SED turns over in the Lyman edge region (see Fig. 22). As discussed in § 4.1, this may be a way of explaining the red SEDs observed in quasars. However, a quantitative fit was not achieved, and the predicted polarization rise is not as steep as observed. Moreover, they were unable to explain the very steep rise observed in PG 1630+377 (Koratkar

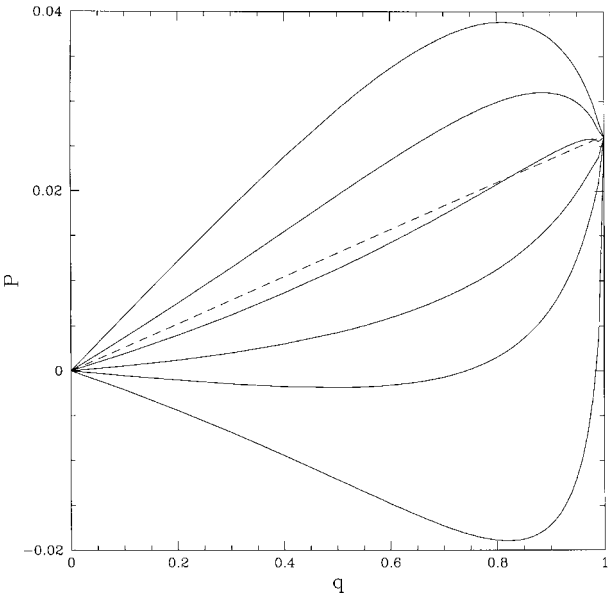

FIG. 21.—Polarization as a function of the ratio of scattering opacity to total opacity q for various values of the thermal source function gradient β. From bottom to top, the solid curves represent $\beta = 0$, 0.5, 1, 2, 5, and ∞. The dashed line is the approximation used by Laor et al. (1990). The observer inclination angle is 63° for all curves. All curves approach the Chandrasekhar (1960) value for this inclination angle as $q \rightarrow 1$, the pure electron-scattering limit. Positive values of polarization correspond to the plane of polarization being parallel to the disk plane, while negative values correspond to the plane of polarization being parallel to the disk symmetry axis. (figure modified from Agol et al. 1998a).

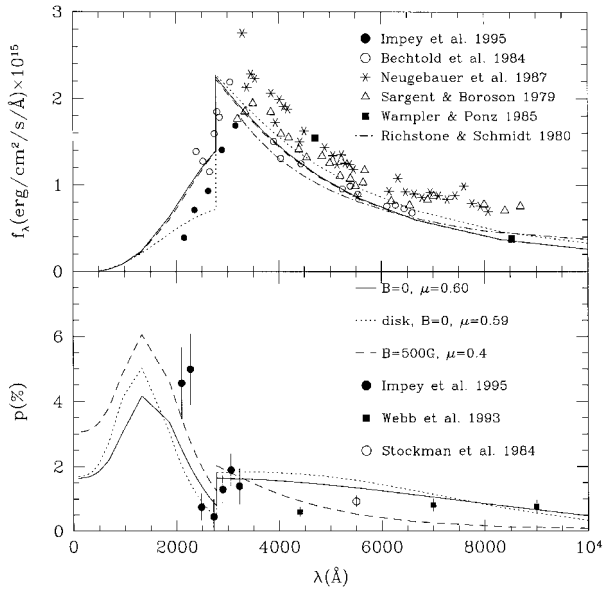

FIG. 22.—Flux and polarization vs. observed wavelength ($z = 2.047$) of PG 1222+228. The solid curve is a fit for a single atmosphere with effective temperature of 20,000 K and surface gravity of 130 cm s^{-2}. The dashed curve shows a fit with the same model but including Faraday rotation effects. Finally, a fit for a standard thin accretion disk model is shown as a short dashed line (from Blaes & Agol 1996).

et al. 1995). In addition, they neglected the relativistic transfer function, which tends to smear and reduce the polarization rise (Agol 1997; Shields, Wobus, & Husfeld 1998), although this may not be a problem if the optically thick portion of the disk does not extend all the way down to the innermost stable orbit.

Shields et al. (1998) have produced a model that produces excellent quantitative agreement with the observations of steep polarization rises near the Lyman edge but is based on ad hoc assumptions. They assume that at every radius the disk produces a spectrum with a sharp Lyman edge in absorption, together with a large Lyman polarization edge in emission. In particular, the polarization is assumed to be zero redward of the edge and an arbitrarily high multiple of the Chandrasekhar (1960) pure electron-scattering polarization blueward of the edge. These spectra are then passed through the relativistic transfer function and can be made to fit the observations quantitatively with few free parameters (see Fig. 23). This is a considerable achievement, but it relies on having a large intrinsic polarization jump at the Lyman limit from the disk. Shields et al. suggest that this might be produced by Lyman continuum photons emitted and scattered by an optically thin, ionized region of the accretion disk, but this remains to be demonstrated. The relativistic transfer function is crucial to their fits, and they require the disk to be viewed nearly edge-on (all their successful fits had inclination angles greater than 75°). The Blaes & Agol (1996) models also required rather large inclination angles (53°–66°).

One of the more successful theoretical solutions to the Lyman edge problem in total flux has been Comptonization of the intrinsic disk spectrum by a corona. Comptonization will of course imprint its own polarization signature on the emerging spectrum. Hsu & Blaes (1998) have presented radiative transfer calculations of Compton scattering of polarized radiation in two-phase accretion disk models with plane-parallel geometry. For featureless spectra, Compton scattering generally produces less polarization than Thomson scattering with the same optical depth. Nevertheless, when Compton scattering is sufficient to smear out a Lyman edge, it generally produces significant polarization in the overall spectrum. Interestingly, Compton scattering can produce very large polarizations *parallel to the disk axis* blueward of an input Lyman edge, and at the same time the edge is smeared out in total flux. However, the rise in polarization magnitude is not steep enough to explain the rises observed in several QSOs (see § 3.3).

Lee & Blandford (1997) suggested that resonance line scattering by an externally illuminated slab may explain the high polarization seen shortward of the Lyman edge in PG 1630+377. To test this model further, we need high-resolution spectropolarimetry in the rest wavelength range 500–1000 Å.

It may in fact be that optical/UV radiation emerging from

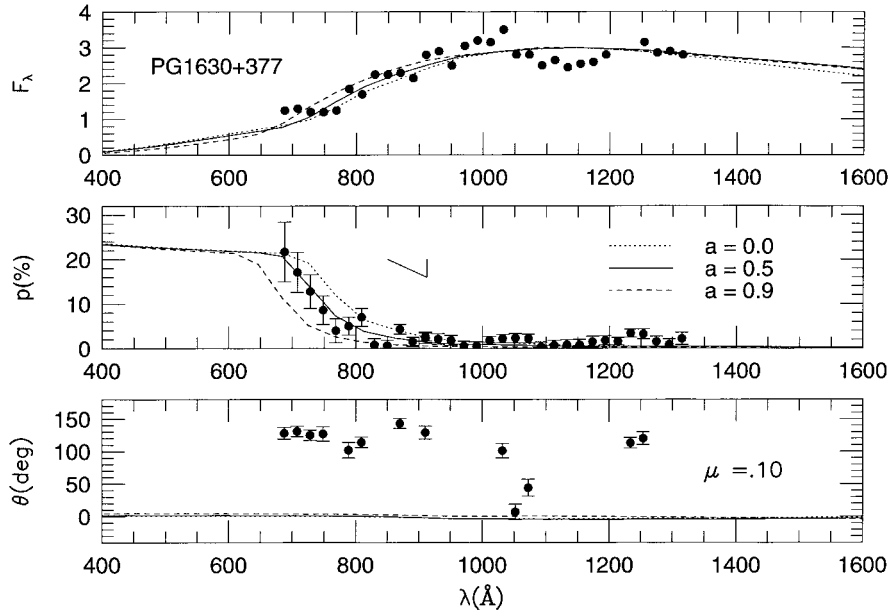

FIG. 23.—Flux (*top*), degree of polarization (*middle*), and polarization position angle (*bottom*) model fits to the observed data of PG 1630+377, from Shields et al. (1998). The position angle of the accretion disk axis is unknown, so the overall offset in angle in the bottom figure is not significant. The inclination angle of the disk is assumed to be 84° (nearly edge-on). Different black hole spin parameters a in units of M are shown. The accretion disk models assume a polarization locally emitted by the disk of zero redward of the edge and 4.4, 4.4, and 5.7 times the Chandrasekhar (1960) value blueward of the edge for $a/M = 0$, 0.5, and 0.9 respectively (courtesy G. Shields).

the accretion disks of AGNs exhibits very little polarization. Magnetic fields are widely believed to play an important role in accretion disks, and they can significantly reduce the polarization emerging from the disk photosphere through Faraday rotation (Gnedin & Silant'ev 1978; Blandford 1990; Matt, Fabian, & Ross 1993; Begelman 1994). The Faraday rotation angle at wavelength λ is $\simeq 0.1\tau_{\rm T}(\lambda/5000\ \text{Å})^2(B_\parallel/1\ \text{G})$, where $\tau_{\rm T}$ is the Thomson depth near the scattering photosphere and $B_\parallel$ is the component of field strength along the line of sight. The equipartition field strength in the inner regions of an α disk is $\sim 10^4\ \text{G}\ \alpha^{-1/2}\,(M/10^8\ M_\odot)^{-1/2}$. Hence unless the filling factor of magnetized regions on the disk photosphere is very small, the optical (and UV perhaps) radiation from the disk should be completely depolarized. Detailed polarized radiative transfer calculations through disks with pure electron-scattering atmospheres confirm this (Agol & Blaes 1996). Complications arise when absorption opacity is included, but generally the effect of magnetic fields is still to reduce the overall polarization. The only exception is when the Nagirner effect is present, where modest magnetic fields can actually *increase* polarization (Agol, Blaes, & Ionescu-Zanetti 1998a).

If Faraday rotation or some other process wipes out optical continuum polarization from the accretion disk photosphere, then one must still find an explanation for the small polarization that is actually observed. One possibility is dust and electron scattering in a stratified wind on scales much larger than the central accretion flow. This mechanism is capable of explaining both the large perpendicular polarizations in Seyfert 2 galaxies and the small parallel polarizations in Seyfert 1 galaxies in a manner consistent with unification schemes (Kartje 1995). Thomson scattering in a fast wind near the accretion disk is also capable of producing polarizations parallel to the disk axis (Beloborodov 1998) because relativistic aberration makes the radiation field limb-brightened in the rest frame of the scattering electrons.

The current spectropolarimetric observations place strong constraints on the models. The low polarization observed in AGNs indicates that if electron-scattering–dominated disk atmospheres are considered, then magnetic field effects must be included in the calculations.

5. ALTERNATIVES TO STANDARD ACCRETION DISKS

The geometrically thin disk models we have been discussing so far have been explored most extensively. However, there are good reasons to believe that accretion flows in AGNS may not always (if ever!) adopt such a simple geometry. In this section we discuss the alternatives and point out, where we can, the main observational and theoretical difficulties. However, it should be borne in mind that much more theoretical work needs to be done to enable these models to be compared with observations. In many cases the models have not yet received the theoretical attention necessary to enable them to

address some of the main observational issues discussed in this review.

5.1. Thick Disks

At both low and high accretion rates, it is possible for internal pressure to become just as important as gravity and rotation. The vertical thickness can then become comparable to the radius, which will result in a *thick disk*. Such disks can resemble tori and/or quasi-spherical accretion flows. At high accretion rates, the outward radiation flux saturates near the Eddington limit (Begelman & Meier 1982), and radiation pressure becomes very important and might support a thick disk geometry. Most of the models of radiation pressure–supported thick disks assume that away from the innermost regions, the flow is in hydrostatic equilibrium on an orbital timescale. This necessarily requires that the flow have a low viscosity parameter α, which is simply the ratio of the orbital time to the infall time for geometrically thick flows. Exceedingly low viscosities are also required in order that the flow be optically thick (see, e.g., Rees 1984). Models of radiation-supported thick disks or tori have been constructed by Paczyński & Wiita (1980), Jaroszyński, Abramowicz & Paczyński (1980), and Abramowicz, Calvani, & Nobili (1980). The geometry of such models is determined by their surface distribution of specific angular momentum, which is not known a priori and is presumably determined by the "viscous" angular momentum transport. In addition to the viscosity constraints, such models in their simplest (nonaccreting!) forms may be subject to global hydrodynamical instabilities (Papaloizou & Pringle 1984), which produce strong spiral waves in the flow (Hawley 1991). Accretion through the disk may, however, reduce the effects of these instabilities (Blaes 1987; Gat & Livio 1992; Dwarkadus & Balbus 1996).

There have been very few predictions of the observed properties of radiation-supported thick disks. Madau (1988) has modeled the emerging SED, which has a strong dependence on viewing angle. This is because most of the luminosity originates in the central funnel region, which is shadowed by the outer torus-shaped disk for large viewing angles. Observers who can view the funnel see a spectrum that extends up to the soft X-rays, whereas observers who view the disk more edge-on see a much cooler spectrum. High inclination angles may be required to make the models compatible with observed UV/soft X-ray flux ratios in Seyfert 1 galaxies (Walter & Fink 1993). This may be incompatible with the unified model and low inclination angles inferred from Fe Kα lines, but it should be pointed out that thin disk models have not succeeded in explaining the soft X-ray excess in a self-consistent fashion either. In addition, the optical/UV SED for thick disks suffers the same problem as in thin disks in being bluer than observed. On the other hand, scattering in the funnel provides a way of producing polarization parallel to the radio axis (Coleman & Shields 1990; Kartje & Königl 1991). In addition, because heat diffuses in all directions, not just vertically, all elements of the photosphere are thermally coupled together, and optical and UV radiation might therefore be expected to exhibit correlated variability with no lags (see the discussion by Szuskiewicz, Malkan & Abramowicz 1996), as observed.

5.2. Slim Disks

The usual α-viscosity prescription, in which the viscous stress is proportional to the total (gas plus radiation) pressure, leads to disks that are thermally and viscously unstable in cases in which the accretion rate is high enough that the inner regions of the disk are supported by radiation pressure (see, e.g., Shakura & Sunyaev 1976). Whether such instabilities are real is not at all clear because of the strong dependence on the ad hoc viscosity prescription (see, e.g., Piran 1978). However, if they are real, it may be that the disk jumps to a higher accretion rate, optically thick, geometrically "slim" (not thin) disk, in which the flow is stabilized by advection of heat into the black hole (Abramowicz et al. 1988). Even ignoring such instabilities, thin disk models are inconsistent at accretion rates above 20%–30% of the Eddington rate, where the flow probably adopts a slim disk geometry and advection must be included. Slim disks are essentially the same as the geometrically thick disks discussed above, except that the radial and vertical structure can be modeled separately. In particular, one can still use vertically integrated equations to describe the radial variation of flow variables. At high, super-Eddington accretion rates, this approximation must eventually break down, and the full two-dimensional thick disk equations must be solved (see, e.g., Papaloizou & Szuszkiewicz 1994).

Slim disk models are probably more appropriate for bright AGNs than standard thin disks, but once again, very little work has been done on their predicted SED. Szuszkiewicz et al. (1996) have calculated emergent spectra of slim disks by assuming that each annulus emits as a modified blackbody. Such models therefore make no predictions of discrete features such as the Lyman edge. Within this approximation, slim disk spectra are identical to thin disk spectra at low accretion rates, but at high (super-Eddington) accretion rates, the SED of a slim disk becomes redder in the extreme UV than that of a thin disk model with the same mass and accretion rate. The differences in the optical/UV SED predictions between the thin and slim disk models remain small, and slim disks still do not provide a satisfactory fit to the observations if the infrared bump is indeed due to thermal dust emission. Szuszkiewicz et al. (1996) propose that the optical/UV continuum may arise from reprocessing of radiation from the inner disk, which as noted above is one way out of this difficulty (see § 4). Slim disks do have an advantage over thin disks in that they can produce thermal soft X-rays without being inconsistent, because Eddington or super-Eddington accretion rates are required. Even here though the modified blackbody approximation produces a steeply falling soft X-ray excess, which does not seem to explain the comparatively flat spectra of QSOs. Better atmosphere mod-

eling may provide better agreement. Slim disks might be able to explain the steep soft X-ray excesses observed in narrow line Seyfert 1 galaxies (Szuszkiewicz 1997).

5.3. Advection-dominated Accretion Flows

Provided the accretion rate is not too high, it is possible for the surface density of the disk to be so low that Coulomb interactions alone are not sufficient to maintain thermal coupling between ions and electrons on the infall timescale. Assuming nothing else couples these particles together, then the thermal energy of the ions will not be radiated away and instead may simply be advected into the central black hole. If the gravitational energy released is channeled primarily into the ions, rather than into the electrons, then the ions can become very hot and produce a gas pressure–supported disk with a very low radiative efficiency (Ichimaru 1977; Rees et al. 1982). Such advection-dominated accretion flows (ADAFs) have received considerable attention in recent years, thanks to the seminal work of Abramowicz et al. (1995) and Narayan & Yi (1995), who showed them to be thermally and viscously stable. The connection between the thin disk, slim disk, and two-temperature ADAF solutions as a function of black hole mass, accretion rate, radius, and viscosity parameter has been discussed by Chen et al. (1995).

It is not clear yet whether the two requirements for an ADAF (low thermal coupling between the ions and electrons and predominately ion heating rather than electron heating) can truly be satisfied in a realistic flow. Begelman & Chiueh (1988) have identified unstable plasma modes that could significantly heat electrons in regions of the flow in which a high level of small-scale magnetohydrodynamic turbulence is present. Such modes may destroy the two-temperature structure of an ADAF, especially in AGNs, if collisionless shocks exist in the flow with sufficiently high filling factor (Narayan & Yi 1995). In addition, the magnetohydrodynamic turbulence that drives accretion primarily heats the electrons unless the magnetic field is significantly below equipartition strength (Quataert 1998; Gruzinov 1998; Quataert & Gruzinov 1998).

Two-temperature ADAFs are by definition very inefficient and are therefore most applicable to low-luminosity AGNs. The most successful application of the theory is perhaps to explaining the broadband emission from the Galactic center (Narayan, Yi, & Mahadevan 1995). ADAFs may also serve as useful models of X-ray–emitting coronae in brighter AGNs.

5.4. Warped Disks

Accretion disks may not be flat in shape. If the angular momentum of the flow is misaligned with the spin axis, then the disk will be warped in such a way as to allow the inner parts to lie in the equatorial plane of the hole (Bardeen & Petterson 1975). It may be that the radiation-induced warping instability (Pringle 1997) could extend to the inner regions of accretion disks or that other warping modes exist there (see, e.g., Marković & Lamb 1998). Such warping would immediately produce less overall polarization in the direct emitted spectrum, owing to the breaking of plane-parallel geometry (cf. the surface irregularities discussed by Coleman & Shields 1990). However, it would also open the possibility of scattering of optical/UV radiation by different parts of the disk, thereby producing different polarization signatures. In addition, if a warped disk intercepts and reprocesses radiation from the inner regions, the effective temperature distribution could flatten from the canonical $T_{\rm eff} \propto r^{-3/4}$ to $r^{-1/2}$, which would produce a long-wavelength SED of $F_\nu \propto \nu^{-1}$, much redder than the canonical $\nu^{1/3}$ distribution, and perhaps more in line with observations. The theoretical problem of the spectral and polarization properties of the radiation emerging from a warped disk in an AGN remains to be explored.

5.5. Optically Thin Emission and Multiphase Flows

The problems with accretion disk models have led some authors to propose optically thin emission as a possible explanation for the BBB. The simplest model is simply free-free emission in an optically thin plasma (see, e.g., Barvainis 1993), possibly powered by reprocessing of X-rays or by direct mechanical heating. Reprocessing of X-rays into BBB photons by cool, optically thin clouds has been considered by many authors (Ferland & Rees 1988; Ferland, Korista, & Peterson 1990; Celotti, Fabian, & Rees 1992; Collin-Souffrin et al. 1996; Kuncic, Celotti, & Rees 1997). Optically thin emission is of course also accompanied by substantial line and edge features, but just as in disks (see, e.g., Kriss 1994), Comptonization and relativistic smearing might help to reduce them in the observed SED.

The inner regions of accretion disks themselves may be very inhomogeneous and exist in a multiphase flow consisting of clouds in a hot, magnetized intercloud medium. Krolik (1998) has proposed that such an equilibrium would be both thermally and viscously stable, in contrast to the standard radiation pressure–supported thin disk with the usual α-viscosity. Gammie (1998) has found that magnetized, radiation pressure supported disks are likely to suffer from a *dynamical* photon bubble instability, which might in fact lead to just such a multiphase equilibrium.

As we noted in § 4.1, the real problem facing accretion disk models may be in explaining the origin of the ionizing continuum. In addition to the usual disk and hot, Comptonizing corona, Magdziarz et al. (1998) have invoked a third phase to explain the EUV and soft X-rays in NGC 5548: a warm (~0.3 keV), optically thick Comptonizing medium (see Fig. 24). This component is reminiscent of models of the soft X-ray excess that invoke thermal Comptonization in the inner regions of the accretion disk itself (Czerny & Elvis 1987; Maraschi & Molendi 1990; Ross et al. 1992; Shimura & Takahara 1993, 1995; Dörrer et al. 1996). Note that Zheng et al.'s (1997) interpretation of the EUV/soft X-ray component in the *HST*

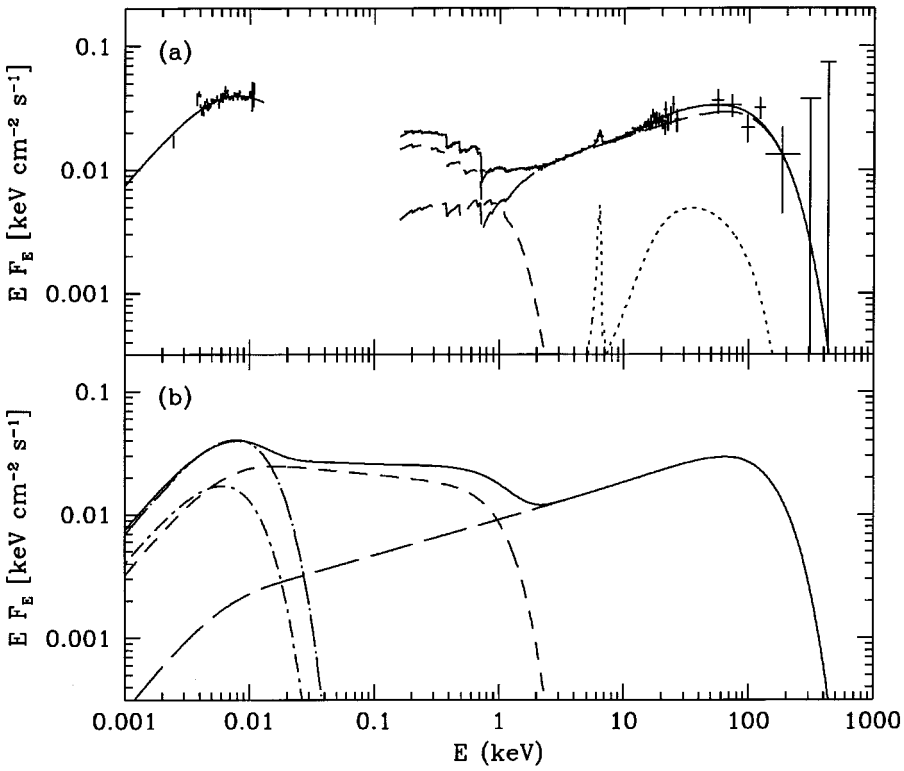

FIG. 24.—Broadband average spectrum of NGC 5548, from simultaneous archival optical/*IUE*/*Ginga* data, as well as nonsimultaneous *ROSAT* and *GRO*/OSSE data. The upper panel shows the data and fitted model, while the lower panel shows a decomposition of the spectrum into disk and thermal Comptonization continuum components. The dot–short-dashed curve shows the disk, modeled using blackbodies. The short-dashed curve is the soft excess component, modeled with thermal Comptonization in an optically thick, warm medium. This component dominates the spectrum from the optical/UV to 1 keV. The long-dashed and dotted curves show the hot thermal Comptonization and reflection components, respectively. The dot–long-dashed curve shows the disk component fitted to the optical/*IUE* data separately and is analogous to the cool disk fit to the composite spectrum shown in Fig. 17 (from Magdziarz et al. 1998).

composite was also based on Comptonization but in a hotter, more optically thin medium. The geometry of the three components is very unclear, however. A thermal Comptonization origin would be one way of getting rid of the Lyman edge in this Seyfert galaxy. In addition, it provides another interpretation of the fact that the optical/UV component becomes harder when brighter—here the disk component could be constant, while the soft excess component becomes brighter. Much more work needs to be done on theoretical models of such multiphase flows.

6. SUMMARY AND DIRECTIONS FOR THE FUTURE

In this section we summarize the observational and theoretical facts of accretion disks in AGNs and suggest a few directions for future work. Once again, we emphasize that we have concentrated on radio-quiet AGNs.

The optical/UV continuum slopes are redder than predicted by most luminous thin disk models whose spectra extend to the extreme ultraviolet. Bare accretion disks that produce substantial numbers of ionizing photons generally have optical/UV SEDs that are too blue.

The UV and X-ray composite spectra indicate that the BBB may not be as energetically dominant as thought previously. However, in both Seyfert galaxies and QSOs, there are individual objects that show a large range in BBB properties. Intrinsic reddening, geometry, etc. may also play an important role in modifying the BBB SED. Therefore, it is possible that the intrinsic BBB SED is very different from the observed BBB SED. There has not yet been a systematic study of a "complete" sample of AGNs over a wide wavelength range to determine the range of BBB properties.

Intrinsic Lyman edges that can be associated with accretion disks are rare in AGNs. More importantly, Lyman edges have never been seen in emission. Although the new accretion disk calculations demonstrate that the strength of the Lyman edge feature is not nearly as strong as thought in the earlier models, getting rid of the Lyman edge is difficult.

Both Seyfert galaxies and QSOs show very low optical polarization. QSOs also show low UV polarization (up to 1000 Å), and there seems to be no wavelength dependence in

the polarization signature. The low polarization indicates that a simple geometrically thin, optically thick accretion disk with pure electron-scattering opacity is ruled out, unless magnetic fields are invoked to reduce the polarization through Faraday rotation. A handful of QSOs have shown a wavelength -dependent polarization shortward of the Lyman edge, but as yet there is no satisfactory theoretical model that explains these observations.

The spectropolarimetric observations provide information along a different sight line to the nucleus and hence provide clues to the geometry of this region. Obtaining high signal-to-noise ratio data is time-consuming, but when such data are obtained, they place strong constraints on the disk geometry, atmosphere, emission mechanism, and magnetic fields. Hence these observations are essential to understanding the accretion disks of AGNs.

Fe Kα emission lines with a range of properties have been observed in Seyfert galaxies, but no such observations exist for QSOs. Although the Fe Kα line indicates the presence of an accretion disk, a full multiwavelength theoretical interpretation has been undertaken for only one object.

X-rays are an important contributor to the bolometric luminosity of low-luminosity AGNs (Seyfert galaxies), and there are strong indications that at least some of the optical/UV arises from reprocessing of the X-rays, which in turn feed back through Compton scattering to produce the X-rays themselves. Variability campaigns such as the recent one on NGC 7469 indicate that this reprocessing is more complex than anticipated. Nevertheless, it is clear that X-rays play an energetically important role, and they will clearly modify the properties of the optical/UV emitting plasma. Sophisticated, self-consistent calculations of the atmosphere structure and optical/UV/X-ray radiative transfer through illuminated accretion disks need to be performed. Also, high time resolution variability monitoring campaigns that span a large wavelength region are once more essential to our understanding of the emission mechanism in AGNs.

Variability data also show that the optical/UV continuum slope is bluer when the object is brighter. Variations in the accretion rate of a cool bare disk can explain this, but they may also indicate a variation in the luminosity from a separate, EUV/soft X-ray–emitting phase of the flow.

The Einstein Cross provides a unique probe of the central emitting regions of this particular QSO. Monitoring of this source has already placed severe constraints on the size scale of the *optical* emitting regions, which may be problematic for accretion disk models. Multicolor photometric monitoring of this source should be continued in the optical and in fact in other wave bands to strengthen these constraints. Such observations complement variability campaigns in other sources in probing the geometry and size of the inner accretion flow.

Sophisticated atmosphere modeling is now being applied to the accretion disks of AGNs to improve on the naive blackbody assumption. However, once one leaves the blackbody prescription, then the vertical density and temperature structure must be specified. Unfortunately, this is likely to remain very uncertain for some time to come, until the viscous transport of angular momentum is better understood. Ultimately, radiative transfer calculations coupled with the results of magnetohydrodynamic simulations may be necessary to put the theory on somewhat firmer (i.e., based on first principles) ground. Even assuming the vertical structure can be calculated, atmosphere calculations need to be improved to include non-LTE effects, Compton scattering, and opacity from metals—particularly metal lines, in a self-consistent way. No models exist as yet which do this.

The assumptions of the standard thin accretion disk are inconsistent at high luminosities, and the sophisticated atmosphere models need to be applied to slim disks.

The dynamics and thermodynamics of magnetized, radiation-supported accretion flows need to be better understood. Is an accretion disk a good description of such flows, or are they broken up into a complex, multiphase medium?

The possibility of reprocessing of photons from the inner disk or corona by an outer warped, flared, or ruffled disk needs to be explored.

A better understanding of jet formation in AGNs can also contribute to an understanding of disks. The Galactic black hole sources (e.g., GRS 1915+105; Mirabel et al. 1998) are nearby objects that will be extremely useful to study in detail.

To really test accretion disk models requires high signal-to-noise ratio observational data that cover all the energetically important (X-ray, far-UV, and the UV/optical) wave bands. Only then can the Fe Kα emission line, the BBB region, and the Lyman limit region all be investigated simultaneously. Further, variability constraints indicate the need for simultaneous or near-simultaneous observations from the optical to hard X-ray bands. Monitoring campaigns to understand the nature of the correlations between the spectral wave bands are also essential.

Another important observational criterion must be the choice of targets. Given the various parameters that can influence the theoretical calculations, the sample needs to be carefully selected. The objects must have a reasonably clean line of sight so that observational difficulties can be minimized and high signal-to-noise ratio data can be effectively and efficiently obtained. Although AGNs are known to be similar across many orders in luminosity, there are/may be differences that could indicate subtle variations in the nature of the central power house, dependent on luminosity. Therefore, observations must include objects that span the the luminosity range of AGNs. Then accretion disk structure can be discussed as a function of luminosity. Currently, many observational facts are used to try and constrain accretion disk theory without regard to the fact that these constraints arise from AGNs with different luminosities.

The present generation of telescopes (*HST, RXTE, ASCA*) and the telescopes that will be flying in the next few years

(*FUSE*, *XMM*) provide us with an opportunity to obtain high spectral resolution observations of the BBB in a complete sample of AGNs.

Theoretical models of the accretion flow are still primitive and ultimately must deal with at least four components: the dynamics and thermodynamics of a turbulent, magnetized flow; radiative transfer through that flow; Comptonization in both a hot corona and perhaps an intermediate phase to explain the EUV/soft X-ray ionizing continuum; and probably also high-energy emission from a jet or other outflow. There are observational indications that multiphase models and geometry are important, and these need to be explicitly considered in future theoretical models.

We thank E. Agol, R. Antonucci, A. Frey, C.-M. Hsu, I. Hubeny, A. Kinney, J. Krolik, J. Pringle, and G. Shields for useful discussions. We also thank E. Agol, I. Hubeny, A. Laor, K. Nandra, D. Reimers, M. Sincell, W. Welsh, and W. Zheng for supplying data and figures. E. Agol, S. Collin, A. Laor, M. Livio, G. Shields, and P. Stockman supplied comments that greatly improved the paper. This work was supported by NSF grant AST 95-29230, NASA grant NAG5-7075, and *HST* GO grants GO-6109 and GO-6705 provided by the Space Telescope Science Institute, which is operated by the Association of Universities for research in Astronomy Inc., under NASA contract NAS 5-26555.

REFERENCES

Abramowicz, M. A., Calvani, M., & Nobili, L. 1980, ApJ, 242, 772
Abramowicz, M. A., Chen, X., Kato, S., Lasota, J.-P., & Regev, O. 1995, ApJ, 438, L37
Abramowicz, M. A., Czerny, B., Lasota, J. P., & Szuszkiewicz, E. 1988, ApJ, 332, 646
Abramowicz, M. A., Lanza, A., & Percival, M. J. 1997, ApJ, 479, 179
Agol, E. 1997, Ph.D. thesis, Univ. of California at Santa Barbara
Agol, E., & Blaes, O. 1996, MNRAS, 282, 965
Agol, E., Blaes, O., & Ionescu-Zanetti, C. 1998a, MNRAS, 293, 1
Agol, E., Hubeny, I., & Blaes, O. 1998b, in AIP Conf. Proc. 431, Accretion Processes in Astrophysical Systems: Some Like It Hot, ed. S. S. Holt & T. R. Kallman (Woodbury, NY: AIP), 175
Alloin, D., Pelat, D., Phillips, M., & Whittle, M. 1985, ApJ, 288, 205
Antonucci, R. 1988, in Supermassive Black Holes, ed. M. Kafatos (Cambridge: Cambridge Univ. Press), 26
———. 1993, ARA&A, 31, 473
Antonucci, R., Geller, R., Goodrich, R. W., & Miller, J. S. 1996, ApJ, 472, 502.
Antonucci, R., Kinney, A. L., & Ford, H. C. 1989, ApJ, 342, 64
Balbus, S. A., & Hawley, J. F. 1991, ApJ, 376, 214
———. 1998, Rev. Mod. Phys., 70, 1
Bardeen, J. M., & Petterson, J. A. 1975, ApJ, 195, L65
Barvainis, R. 1987, ApJ, 350, 537
———. 1990, ApJ, 353, 419
———. 1993, ApJ, 412, 513
Bechtold, J., et al. 1994, AJ, 108, 374
Begelman, M. C. 1994, in ASP Conf. Ser. 54, The Physics of Active Galaxies, ed. G. V. Bicknell, M. A. Dopita, & P. J. Quinn (San Francisco: ASP), 51
Begelman, M. C., & Chiueh, T. 1988, ApJ, 332, 872
Begelman, M. C., & Meier, D. L. 1982, ApJ, 253, 873
Beloborodov, A. M. 1998, ApJ, 496, L105
Berriman, G., Schmidt, G. D., West, S. C., & Stockman, H. S. 1990, ApJS, 74, 869.
Blaes, O. M. 1987, MNRAS, 227, 975
Blaes, O., & Agol, E. 1996, ApJ, 469, L41
Blandford, R. D. 1990, in Active Galactic Nuclei, ed. T. J.-L. Courvoisier & M. Mayer (Berlin: Springer), 219
Blandford, R. D., & Payne, D. G. 1982, MNRAS, 199, 883
Blundell, K. M., & Beasley, A. J. 1998, MNRAS, in press
Bochkarev, N., Karitskaya, E. A., & Sakhibullin, N. A. 1985, Ap&SS, 108, 15
Bower G. A., et al. 1997, ApJ, 492, L111
Braatz, J. A., Wilson, A. S., & Henkel, C. 1997, ApJS, 110, 321
Celotti, A., Fabian, A. C., & Rees, M. J. 1992, MNRAS, 255, 419
Chandrasekhar, S. 1960, Radiative Transfer (New York: Dover)
Chen, K., & Halpern, J. P. 1989, ApJ, 344, 115
Chen, K., Halpern, J. P., & Filippenko, A. V. 1989, ApJ, 339, 742
Chen, X., Abramowicz, M. A., Lasota, J.-P., Narayan, R., & Yi, I. 1995, ApJ, 443, L61
Clavel, J., et al. 1992, ApJ, 393, 113
Coleman, H., & Shields, G. 1990, ApJ, 363, 415
———. 1993, Rev. Mexicana Astron. Astrofis., 27, 95
Collier, S. J., et al. 1998, ApJ, 500, 162
Collin, S. & Dumont, A. M. 1997, in Lecture Notes in Physics, 487, Accretion Disks: New Aspects, ed. E. Meyer-Hoffmeister & H. C. Spruit (Berlin: Springer), 216
Collin-Souffrin, S. 1987, A&A, 179, 60
———. 1991, A&A, 249, 344
Collin-Souffrin, S., Czerny, B., Dumont, A.-M., & Życki, P. 1996, A&A, 314, 393
Corrigan, R. T., et al. 1991, AJ, 102, 34
Courvoisier, T. J.-L., & Clavel, J. 1991, A&A, 248, 389
Crenshaw, M., et al. 1996, ApJ, 470, 322
Cunningham, C. T. 1975, ApJ, 202, 788
———. 1976, ApJ, 208, 534
Cutri, R. M., Wiśniewski, W. Z., Rieke, G. H., & Lebofsky, M. J. 1985, ApJ, 296, 423
Czerny, B., & Dumont, M. A. 1998, A&A, in press
Czerny, B., & Elvis, M. 1987, ApJ, 321, 305
Czerny, B., Jaroszyński, M., & Czerny, M. 1994, MNRAS, 268, 135
Czerny, B., & Pojmański, G. 1990, MNRAS, 245, 1P
Czerny, B., & Zbyszewska, M. 1991, MNRAS, 249, 634
Dörrer, T., Riffert, H., Staubert, R., & Ruder, H. 1996, A&A, 311, 69
Dumont, A. M., & Collin-Souffrin, S. 1990a, A&A, 229, 302
———. 1990b, A&A, 229, 313
Dwarkadus, V. V., & Balbus, S. A. 1996, ApJ, 467, 87
Eardley, D. M., & Lightman, A. P. 1975, ApJ, 200, 187
Edelson, R. A., et al. 1996, ApJ, 470, 364
Eracleous, M. 1998, in ASP Conf. Proc., Structure and Kinematics of Quasar Broad Lines Regions, ed. C. M. Gaskell et al. (San Francisco: ASP), in press
Eracleous, M., & Halpern, J. P. 1994, ApJS, 90, 1
Ferland, G. J., & Rees, M. J. 1988, ApJ, 332, 141
Ferland, G. J., Korista, K. T., & Peterson, B. M. 1990, ApJ, 363, L21
Ford H. C., et al. 1994, ApJ, 435, L27
Ford H. C., Tsvetanov, Z. I., Farrarese, L., & Jaffe, W. 1998, in IAU Symp. 184, The Central Regions of the Galaxy and Galaxies, ed. Y. Sofue (Dordrecht: Kluwer), 377

Francis, P. J., Hewett, P. C., Foltz, C. B., Chaffee, F. H., Weymann, R. J., & Morris, S. L. 1991, ApJ, 373, 465
Gammie, C. F. 1998, MNRAS, 297, 929
Gat, O., & Livio, M. 1992, ApJ, 396, 542
George, I. M., Turner, T. J., Netzer, H., Nandra, K., Mushotzky, R. F., & Taqoob, T. 1998, ApJS, 114, 73
Givon, U., Maoz, D., Kaspi, S., Netzer, H., Smith, P. S., & Jannuzi, B. T. 1998, MNRAS, submitted
Gnedin, Yu. N., & Silant'ev, N. A. 1978, Soviet Astron., 22, 325
Gondek, D., Zdziarski, A. A., Johnson, W. N., George, I. M., McNaron-Brown, K., Magdziarz, P., Smith, D., & Gruber, D. E. 1996, MNRAS, 282, 646
Green, A. R., McHardy, I. M., & Lehto, H. J. 1993, MNRAS, 265, 664
Greenhill, L. J., Jiang, D. R., Moran, J. M., Reid, M. J., Lo, K. Y., & Claussen, M. J. 1995, ApJ, 440, 619
Gruzinov, A. V. 1998, ApJ, 501, 787
Haardt, F., & Maraschi, L. 1991, ApJ, 380, L51
Haas, M., Chini, R., Meisenheimer, K., Stickel, M., Dietrich, L., Klaas, U., & Kreysa, E. 1998, ApJ, 503, L113
Harms, R., et al. 1994, ApJ, 435, L35
Harrington, J. P. 1969, Astrophys. Lett., 3, 165
Hawley, J. F. 1991, ApJ, 381, 496
Hsu, C.-M., & Blaes, O. 1998, ApJ, 506, 658
Hubeny, I., & Hubeny, V. 1997, ApJ, 484, L37
———. 1998, in AIP Conf. Proc. 431, Accretion Processes in Astrophysical Systems: Some Like It Hot, ed. S. S. Holt & T. R. Kallman (Woodbury, NY: AIP) 171
Huchra, J., Gorenstein, M., Kent, S., Shapiro, I., Smith, G., Horne, E., & Perley, R. 1985, AJ, 90, 691
Hughes, D. H., Robson, E. I., Dunlop, J. S., & Gear, W. K. 1993, MNRAS, 263, 607
Hunt, L. K., Zhekov, S., Salvati, M., Mannucci, F., & Stanga, R. M. 1994, A&A, 292, 67
Ichimaru, S. 1977, ApJ, 214, 840
Impey, C. D., Malkan, M. A., Webb, W., & Petry, C. G. 1995, ApJ, 440, 80
Irwin, M. J., Webster, R. L., Hewett, P. C., Corrigan, R. T., & Jedrzejewski, R. I. 1989, AJ, 98, 1989
Iwasawa, K., & Taniguchi, Y. 1993, ApJ, 413, L15
Jaffe, W., Ford, H., Farrarese, L., Van den Bosch, F., & O'Connell, R. 1996, ApJ, 460, 214
Jaroszyński, M., Abramowicz, M. A., & Paczyński, B. 1980, Acta Astron., 30, 1
Jaroszyński, M., Wambsganss, J., & Paczyński, B. 1992, ApJ, 396, L65
Kartje, J. F. 1995, ApJ, 452, 565
Kartje, J. F., & Königl, A. 1991, ApJ, 375, 69
Kaspi, S., et al. 1996, ApJ, 470, 336
Kinney, A. L. 1994, in ASP Conf. Ser. 54, The First Stromlo Symposium: The Physics of Active Galaxies, ed. G. V. Bicknell, M. A. Dopita, & P. J. Quinn (San Francisco: ASP), 61
Kolykhalov, P. I., & Sunyaev, R. A. 1984, Adv. Space Res., 3, 249
Koratkar, A., Antonucci, R. R. J., Goodrich, R. W., Bushouse, H., & Kinney, A. L. 1995, ApJ, 450, 501
Koratkar, A., Antonucci, R. R. J., Goodrich, R. W., & Storrs, A. 1998, ApJ, 503, 599
Koratkar, A. P., Kinney, A. L., & Bohlin, R. C. 1992, 400, 435
Korista, K., Ferland, G., & Baldwin, J. 1997, ApJ, 487, 555
Kormendy, J., et al. 1996a, ApJ, 459, L57
———. 1996b, ApJ, 473, L91
———. 1997, ApJ, 482, L139
Kriss, G. A. 1994, BAAS, 184, 1308
Kriss, G. A., Espey, B. R., Krolik, J. H., Tsvetanov, Z., Zheng, W., & Davidsen, A. F. 1996, ApJ, 467, 622
Kriss, G., Krolik, J., Grimes, J., Tsvetanov, Z., Zheng, W., & Davidsen, A. 1997, in ASP Conf. Proc. 113, Emission Lines in Active Galaxies: New Methods and Techniques, ed. B. M. Peterson, F.-Z. Cheng, & A. S. Wilson (San Francisco: ASP), 453
Krolik, J. H. 1998, ApJ, 498, L13
———. 1999, Active Galactic Nuclei: From the Central Blackhole to the Galactic Environment (Princeton: Princeton Univ. Press)
Krolik, J. H., Horne, K., Kallman, T. R., Malkan, M. A., Edelson, R. A., & Kriss, G. A. 1991, ApJ, 371, 541
Kuncic, Z., Celotti, A., & Rees, M. J. 1997, MNRAS, 284, 717
Kurucz, R. L. 1979, ApJS, 40, 1
Laor, A. 1990, MNRAS, 246, 369
———. 1992, in AIP Conf. Proc. 254, Testing the AGN Paradigm, ed. S. S. Holt, S. G. Neff, & C. M. Urry (New York: AIP), 155
Laor, A., Fiore, F., Elvis, M., Wilkes, B. J., & McDowell, J. C. 1997, ApJ, 477, 93
Laor, A., & Netzer, H. 1989, MNRAS, 238, 897
Laor, A., Netzer, H., & Piran, T. 1990, MNRAS 242, 560
Laor, A., & Draine, B. T. 1993, ApJ, 402, 441
Lee, G., Kriss, G. A., & Davidsen, A. F. 1992, in AIP Conf. Proc. 2540, Testing the AGN Paradigm, ed. S. S. Holt, S. G. Neff, & C. M. Urry (New York: AIP), 159
Lee, H.-W., & Blandford, R. 1997, MNRAS, 288, 19L
Leighly, K. M., et al. 1997, ApJ, 483, 767
Lightman, A. P., & Shapiro, S. L. 1975, ApJ, 198, L73
Livio, M. 1997, in ASP Conf. Ser. 121, Accretion Phenomenon and Related Outflows, ed. D. T. Wickramasinghe, L. Ferrario, & G. V. Bicknell (San Francisco: ASP), 845
Livio, M., & Xu, C. 1997, ApJ, 478, L63
Loskutov, V. M., & Sobolev, V. V. 1979, Astrophyzika, 15, 162
MacAlpine, G. M. 1981, ApJ, 251, 465
MacAlpine, G. M., Davidson, K., Gull, T. R., & Wu, C.-C. 1985, ApJ, 294, 147
Macchetto, F., Marconi, A., Axon, D. J., Capetti, A., & Sparks, W. 1997, ApJ, 489, 579
Madau, P. 1988, ApJ, 327, 116
Magorrian, J., et al. 1998, AJ, 115, 2285
Magdziarz, P., Blaes, O. M., Zdziarski, A. A., Johnson, W. N., & Smith, D. A. 1998, MNRAS, in press
Malkan, M. A. 1983, ApJ, 268, 582
Malkan, M. A., Gorjian, V., & Tam, R. 1998, ApJS, 117, 25
Marković, D., & Lamb, F. K. 1998, ApJ, 507, 316
Marsh, T. R., & Horne, K. 1988, MNRAS, 235, 269
Maraschi, L., & Molendi, S. 1990, ApJ, 353, 452
Masnou, J. L., Wilkes, B. J., Elvis, M., McDowell, J. C., & Arnaud, K. A. 1992, A&A, 253, 35
Mathews, W. G., & Ferland, G. J. 1987, ApJ, 323, 456
Matt, G. 1998, in High Energy Processes in Accreting Black Holes, ed. J. Poutanen & R. Svensson, in press
Matt, G., Fabian, A. C., & Ross, R. R. 1993, MNRAS, 264, 839
Mészáros, P., & Ostriker, J. P. 1983, ApJ, L59
Mirabel, I. F., Dhawan, V., Chaty, S., Rodriguez, L. F., Marti, J., Robinson, C. R., Swank, J., & Geballe, T. R. 1998, A&A, 330, L9
Molendi, S., Maraschi, L., & Stella, L. 1992, MNRAS, 255, 27
Mushotzky, R. F., Done, C., & Pounds, K. A. 1993, ARA&A, 31, 717
Mushotzky, R. F., Fabian, A. C., Iwasawa, K., Kunieda, H., Matusoka, M., Nandra, K., & Tanaka, Y. 1995, MNRAS, 272, L9
Nadeau, D., Yee, H. K. C., Forrest, W. J., Garnett, J. D., Ninkov, Z., & Pipher, J. L. 1991, ApJ, 376, 430
Nakai, N., Inoue, M., & Miyoshi, M. 1993, Nature, 361, 45

Nandra, K., Fabian, A. C., Brandt, W. N., Kunieda, H., Matsuoka, M., Mihara, T., Ogasaka, Y., & Terashima, Y. 1995, MNRAS, 276, 1
Nandra, K., George, I. M., Mushotsky, R. F., Turner, T. J., & Yaqoob, T. 1997a, ApJ, 476, 70
———. 1997b, ApJ, 477, 602
———. 1997c, ApJ, 488, L91
Nandra, K., & Pounds, K. A. 1994, MNRAS, 268, 405
Nandra, K., et al. 1998, ApJ, 505, 594
Narayan, R., & Yi, I. 1995, ApJ, 452, 710
Narayan, R., Yi, I., & Mahadevan, R. 1995, Nature, 374, 623
Netzer, H., & Peterson, B. M. 1997, in Astronomical Time Series, ed. D. Maoz, A. Sternberg, & E. M. Leibowitz (Dordrecht: Kluwer), 85
Neugebauer, G., Green, R. F., Matthews, K., Schmidt, M., Soifer, B. T., & Bennet, J. 1987, ApJS, 63, 615
Novikov, I. D., & Thorne, K. S. 1973, in Black Holes, ed. C. De Witt & B. De Witt (New York: Gordon & Breach), 343
O'Brien, P. T., Gondhalekar, P. M., & Wilson, R. 1988, MNRAS, 233, 801
Østensen, R., et al. 1996, A&A, 309, 59
Paczyński, B., & Wiita, P. J. 1980, A&A, 88, 23
Page, D. N., & Thorne, K. S. 1974, ApJ, 191, 499
Papaloizou, J. C. B., & Pringle, J. E. 1984, MNRAS, 208, 721
Papaloizou, J., & Szuszkiewicz, E. 1994, MNRAS, 268, 29
Peterson, B. M. 1993, PASP, 105, 247
———. 1997, An Introduction to Active Galactic Nuclei (Cambridge: Cambridge Univ. Press)
Peterson, B. M., Wanders, I., Horne, K., Collier, S., Alexander, T., Kaspi, S., & Maoz, D. 1998, PASP, 110, 660
Pettersen, B. R. 1990, IAU Circ. 5099
Phinney, E. S. 1989, in Theory of Accretion Disks, ed. W. Duschl, F. Meyer, & J. Frank (Dordrecht: Kluwer), 457
Piran, T. 1978, ApJ, 221, 652
Pounds, K. A., Nandra, K., Stewart, G. C., & Leighly, K. 1989, MNRAS, 240, 769
Pringle, J. E. 1997, MNRAS, 292, 136
Quataert, E. 1998, ApJ, 500, 978
Quataert, E., & Gruzinov, A. 1998, ApJ, submitted
Racine, R. 1991, AJ, 102, 454
———. 1992, ApJ, 395, L65
Rauch, K. P., & Blandford, R. D. 1991, ApJ, 381, L39
Rees, M. 1975, MNRAS, 171, 457
———. 1984, ARA&A, 22, 471
Rees, M. J., Begelman, M. C., Blandford, R. D., & Phinney, E. S. 1982, Nature, 295, 17
Reimers, D., Kohler, S., Hagen, H. -J., & Wisotzki, L. 1998, in Ultraviolet Astrophysics Beyond the *IUE* Final Archive, ed. W. Wamsteker & R. Gonzalez Riestra (Noordwijk: ESA), 579
Richstone, D. 1998, in IAU Symp. 184, The Central Regions of the Galaxy and Galaxies (Dordrecht: Kluwer), 451
Riffert, H., & Herold, H. 1995, ApJ, 450, 508
Ross, R. R., Fabian, A. C., & Mineshige, S. 1992, MNRAS, 258, 189
Salpeter, E. E. 1964, ApJ, 140, 796
Sanders, D. B., Phinney, E. S., Neugebauer, G., Soifer, B. T., & Matthews, K. 1989, ApJ, 347, 29
Sanders, D. B., Scoville, N. Z., & Soifer, B. T. 1988, ApJ, 335, L1
Shakura, N. I., & Sunyaev, R. A. 1973, A&A, 24, 337
———. 1976, MNRAS, 175, 613
Shields, G. 1978, Nature, 272, 706
———. 1989, in Fourteenth Texas Symp. on Relativistic Astrophysics, ed. E. J. Fenyves (New York: NY Academy of Sciences), 110
Shields, G. A., & Coleman, H. H. 1994, in NATO Advanced Research Workshop on Theory of Accretion Disks–2, ed. W. Duschl et al. (Dordrecht: Kluwer), 223
Shields, G. A., Wobus, L., & Husfeld, D. 1998, ApJ, 496, 743
Shimura, T., & Takahara, F. 1993, ApJ, 419, 78
———. 1995, ApJ, 440, 610
Sincell, M. W., & Krolik, J. H. 1997, ApJ, 476, 605
———. 1998, ApJ, 496, 737
Speith, R., Riffert, H., & Ruder, H. 1995, Comput. Phys. Commun., 88, 109
Stockman, H. S., Angel, J. R. P., & Miley, G. K. 1979, ApJ, 227, L55
Stockman, H. S., Moore, R. L., & Angel, J. R. P. 1984, ApJ, 279, 485
Störzer, H., Hauschildt, P. H., & Allard, F. 1994, ApJ, 437, L91
Stone, J. M., Hawley, J. F., Gammie, C. F., & Balbus, S. A. 1996, ApJ, 463, 656
Storchi-Bergmann, T., Eracleous, M., Ruiz, M. T., Livio, M., Wilson, A., & Filippenko, A. V. 1997, ApJ, 489, 87
Sun, W.-H., & Malkan, M. A. 1989, ApJ, 346, 68
Sun, W.-H., Malkan, M. A., & Chang, T. H. W. 1993, BAAS, 25, 1432
Szuszkiewicz, E. 1997, in IAU Colloq. 163, Accretion Phenomena and Related Outflows, ed. D. T. Wickramasinghe, L. Ferrario, & G. V. Bicknell (ASP Conf. Ser. 121) (San Francisco: ASP), 812
Szuszkiewicz, E., Malkan, M. A., & Abramowicz, M. A. 1996, ApJ, 458, 474
Tanaka, Y., et al. 1995, Nature, 375, 659
Turner, T. J., & Pounds, K. 1989, MNRAS, 240, 833
Turner, T. J.., George, I. M., & Mushotzky, R. F. 1993, ApJ, 412, 72
Tytler, D., & Davis, C. 1993, BAAS, 25, 1432
Ulrich, M.-H., Maraschi, L., & Urry, C. M. 1996, ARA&A, 35, 445
Urry, C. M., & Padovani, P. 1995, PASP, 107, 803
van der Marel, R. P., de Zeeuw, P. T., Rix, H. W., & Quinlan, G. D. 1997, Nature, 385, 610
van der Marel R. P., & van den Bosch, F. C. 1998, AJ, submitted
Walter, R., & Fink, H. H. 1993, A&A, 274, 105
Walter, R., Orr, A., Courvoisier, T. J.-L., Fink, H. H., Mikano, F., Otani, C., & Wamsteker, W. 1994, A&A, 285, 119
Wambsganss, J., Schneider, P., & Paczyński, B. 1990, ApJ, 358, L33
Wampler, E. J., & Ponz, D. 1985, ApJ, 298, 448
Wanders, I., et al. 1997, ApJS, 113, 69
Wehrse, R. 1997, in ASP Conf. Ser. 121, Accretion Phenomenon and Related Outflows, ed. D. T. Wickramasinghe, L. Ferrario, & G. V. Bicknell (San Francisco: ASP), 162
Welsh, W. F., Peterson, B. M., Koratkar, A. P., & Korista, K. T. 1998, ApJ, 509, 118
Wills, B., Netzer, H., & Wills, D. 1985, ApJ, 288, 94
Zeldovich, Y. B., & Novikov, I. B. 1964, Dokl. Acad. Nauk SSSR, 158, 811
Zheng, W., et al. 1995, ApJ, 444, 632
Zheng, W., Kriss, G. A., Telfer, R. C., Grimes, J. P., & Davidsen, A. F. 1997, ApJ, 475, 469
Zheng, W., et al. 1999, in preparation